ISSN 1335-8421 Acta Med Mart 2002, 2(3)

ACTA MEDICA MARTINIANA

Journal for Biomedical Sciences, Clinical Medicine and Nursing

Contents

Published by the Jessenius Faculty of Medicine in Martin, Comenius University in Bratislava, Slovakia

Editorial Office:
Acta Medica Martiniana
Jessenius Faculty of Medicine, Comenius University
(Dept. of Physiology)

Malá Hora 4
037 54 Martin
Slovakia

Instructions for authors: http:ll www.jfmed.uniba.sk (Acta Medica Martiniana)

Tlač:
ProKonzult, s. r. o., závod NADAS, Vrútky

MYELIN SHEATH FORMATION. CAN LONGITUDINAL SECTIONS OF THE DEVELOPING NERVE CLARIFY ITS MECHANISM?

Yvetta Mellová, Milan Mello, Desanka Výbohová, Gabriela Hešková, Lenka Kunertová, Magdaléna Marčeková
Department of Anatomy, Comenius University, Jessenius Faculty of Medicine, Martin, Slovak Republic

Abstract

The ultrastructure of the peripheral nerve in young rats was studied to acquire better knowledge about the process of myelin sheath formation.

Myelinating nerve fibers were examined in longitudinal sections of the sciatic nerve in rats during the first 28 days of their postnatal development. Authors focused particularly on the paranodal region of myelinating fibers following changes of terminal loops of myelin lamellae.

The terminal loops in the developing nerve fibers were found being different from the loops found in the adult ones. At the beginning of myelination terminal loops contact the axon at large surface area and they are not connected with it by axoglial junction. Terminal loops change with the increasing number of the myelin lamellae. Their contact surface area with the axon is diminishing and the axoglial junction is being formed. Transformation process in the terminal loops starts in the loops of outer lamellae.

This suggests that outer lamellae are older than inner lamellae. Authors assume that myelin membrane formation is a result of inner mezaxon's growth and that new lamellae develop at the inner surface of the myelin sheath.

Key words: myelination, myelin lamellae, terminal loops, axoglial junction

INTRODUCTION

The process of myelin sheath formation and growth has not been completely known till now, though as early as in 1954 Geren (1) has found that the mezaxon, which is continuous with Schwann cell surface membrane, grows and forms a spiral sheath around the axon. The peripheral nerve development was studied by many authors (2,3,4,5,6,7,8), but the process of axon enveloping and myelin sheath formation itself was in focus only of some of them (9,10,11,12).

The most cited author who made an effort to clarify the process of myelin sheath formation is Webster (9). Webster provided very detailed description of myelinating nerve fibres. Studying serial transverse sections of developing nerves he found that initially the outer edge of mesaxon is relatively fixed while its inner edge remains free to rotate around the axon. Later the length and internal circumference of myelin spiral is becoming larger and the number of turns also increases. Webster (9) concluded – „How this happens remains poorly understand".

We decided to try to complete the knowledge about myelinogenesis studying longitudinal sections of developing peripheral nerves.

METHODS

The sciatic nerves of the youngs of white rat, family Wistar, aged 1 to 28 days of their postnatal development were used to study the ultrastructural changes occurring during the nerve fiber myelination. The peripheral nerves were taken in one-day intervals, from the 1st to 14th day and on the 16th, 19th, 21st and 28th days. Sciatic nerves of two 6 weeks old animals were used as a control material.

In animals under deep pentobarbital anaesthesia (Pentobarbital Spofa Praha, Czechoslovakia). Sciatic nerves were exposed and fixed in situ by 3 % glutaraldehyde

Address for correspondence:
Assoc. Prof. Y. Mellová, M.D., Ph.D., Department of Anatomy, Comenius University, Jessenius Faculty of Medicine, Malá Hora 4, 037 54 Martin, Slovak Republic
Phone: ++421 43 4131 427
e-mail: mellova@jfmed.uniba.sk

(Glutaraldehyde solution, Fluka Chemie AG, Switzerland) in 0.1 M phosphate buffer at pH of 7.4 for 10 minutes. Removed nerves were immersed in the same solution for 3 hours at the temperature of 4° C and postfixed in 1 % osmiumtetroxide (Osmium/VIII/-oxid, Merck). After dehydration through graded alcohols, the tissue was embedded in Durcupan ACM Fluka, BRD. Ultrathin sections were prepared by ultramicrotome (LKB BROMMA, Switzerland) and contrasted by uranylacetate (Lachema Brno, Czechoslovakia) and lead citrate (Merck). The specimens were examined using transmission electron microscope BS 500 (TESLA, Brno Czechoslovakia).

RESULTS

In the longitudinal sections of peripheral nerve on the 1st and 2nd days of postnatal development rare myelinating nerve fibers were found in which the axons were enveloped by compact myelin lamellae. The paranodal region was possible to be seen as late as on the 3rd day after birth, when the number of the myelinating fibers was larger. In the paranodal region of myelinating fibre the myelin sheath lamellae were terminated by large, flat terminal loops, contacting the axon at wide surface area, without being connected with it by axoglial junction (Fig. 1, 2). The appearance of the terminal loops in the myelinating fiber with the first compact lamellae was the same even in the next days. Increasing number of the myelin lamellae was accompanied by changes of terminal loops. Their contact area was diminishing and the axoglial junction appeared. However, all terminal loops of the same paranodal region did not show described changes simultaneously. Smaller contact area with the axon was found in the loops of outer lamellae - lying close to the Ranvier node. And just these loops were the first connected with the axon by axoglial junction. These changes were seen in fibers with higher number of lamellae in the first as well as the following days after the birth (Fig. 3). Big flat terminal loops not connect-

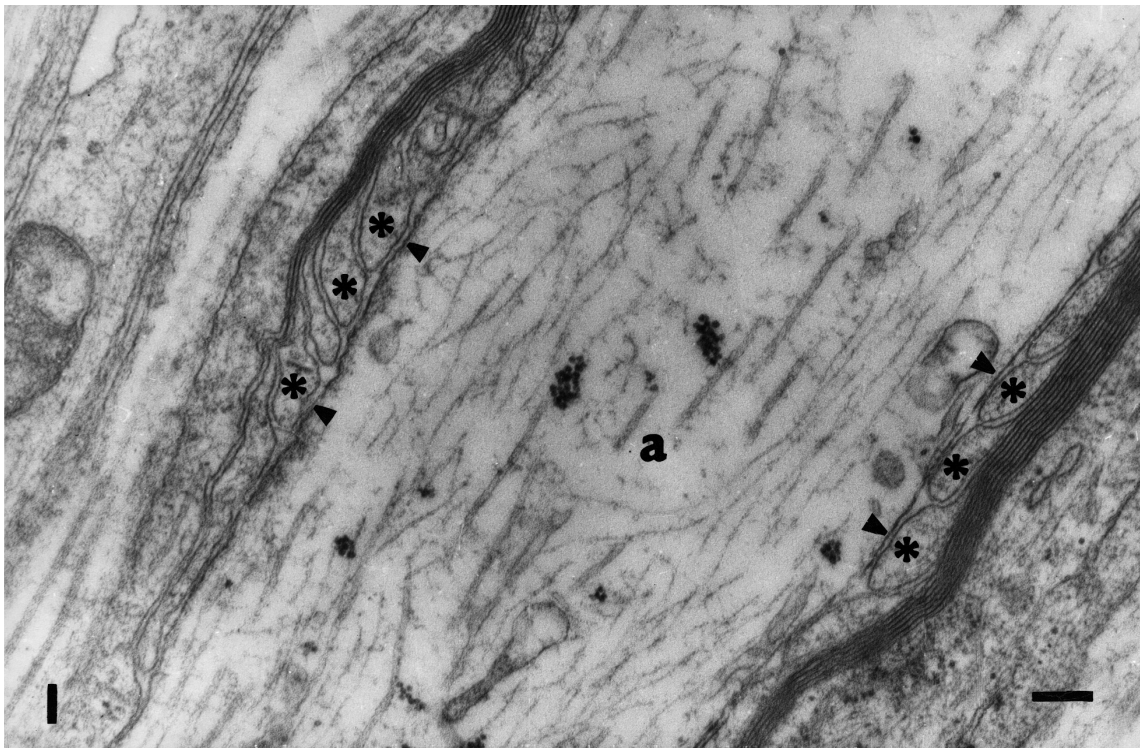

Fig. 1. Myelinating nerve fiber at the 3rd day after the birth. Paranodal region. Myelin lamellae terminate by large terminal loops (asterisks) which are not connected with the axon. Note distinct periaxonal space (arrowhead). Bar, 0.2 μm.

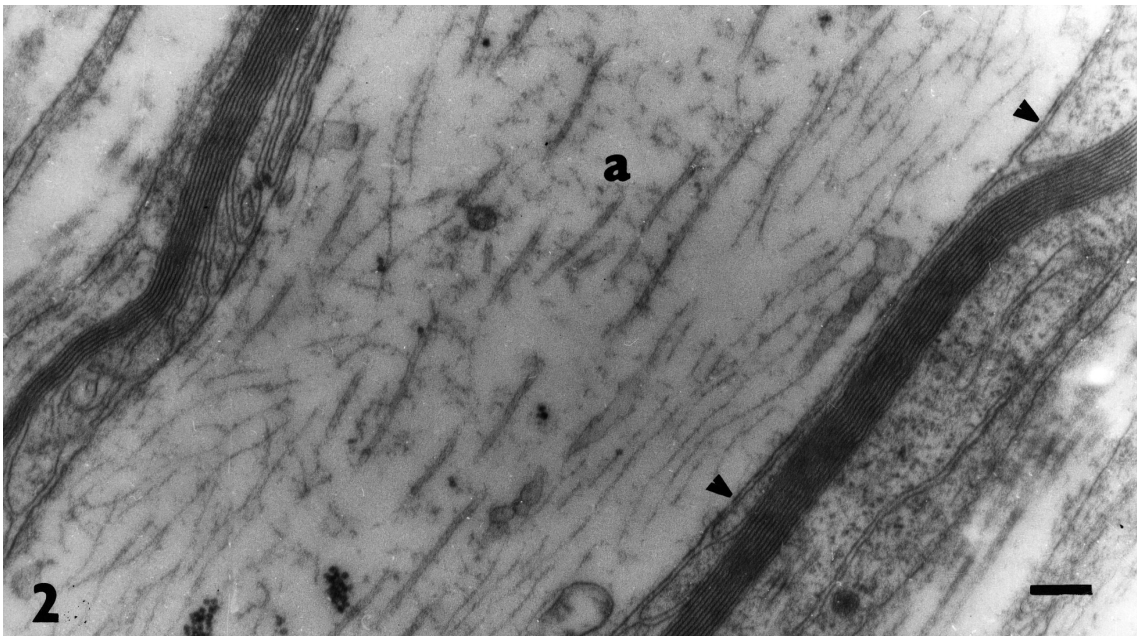

Fig. 2. The same paranodal region - more proximally - towards the centre of internode. Two large terminal loops of inner lamellae are marked by arrowheads. Bar, 0.2 μm

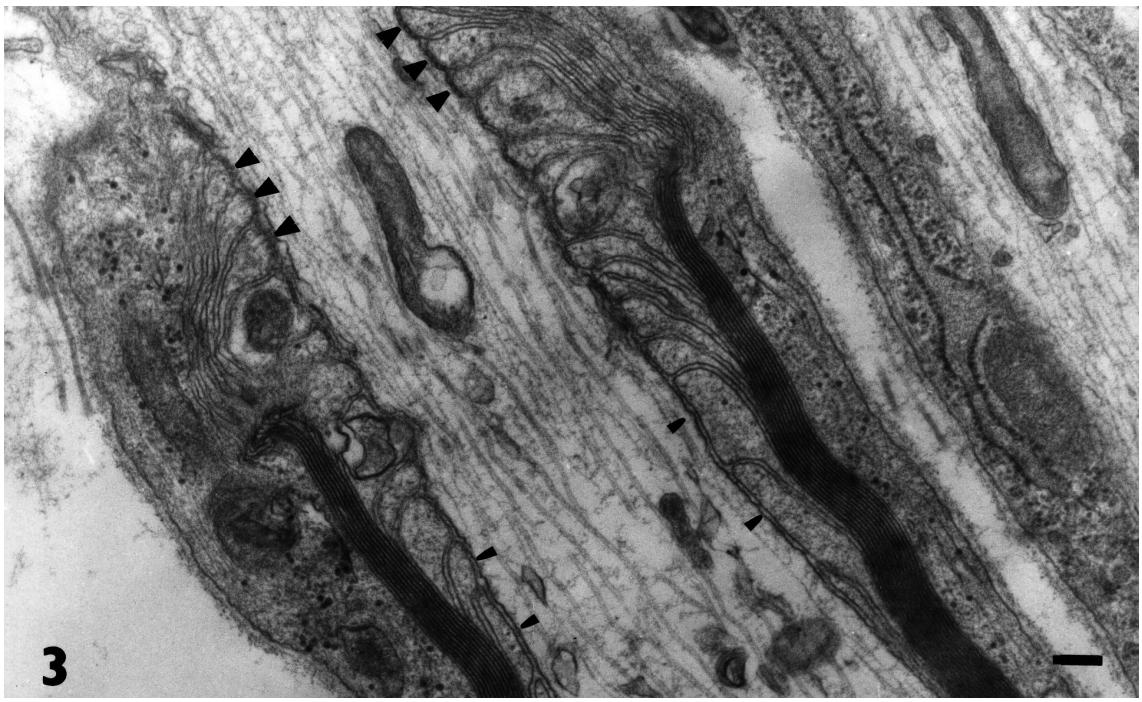

Fig. 3. Advanced process of myelinogenesis - 4th day after the birth. Paranodal region of a fibre enveloped by more than 10 myelin lamellae is shown. Terminal loops of inner lamellae (marked by arrowheads) are large, flat. They are not connected with the axon - note the distinct periaxonal space. Terminal loops of outer lamellae (marked by bold arrowheads) contact the axon by smaller area and are connected with it by axoglial junction seen as a dark points occupying the periaxonal space. Bar, 0.2 μm.

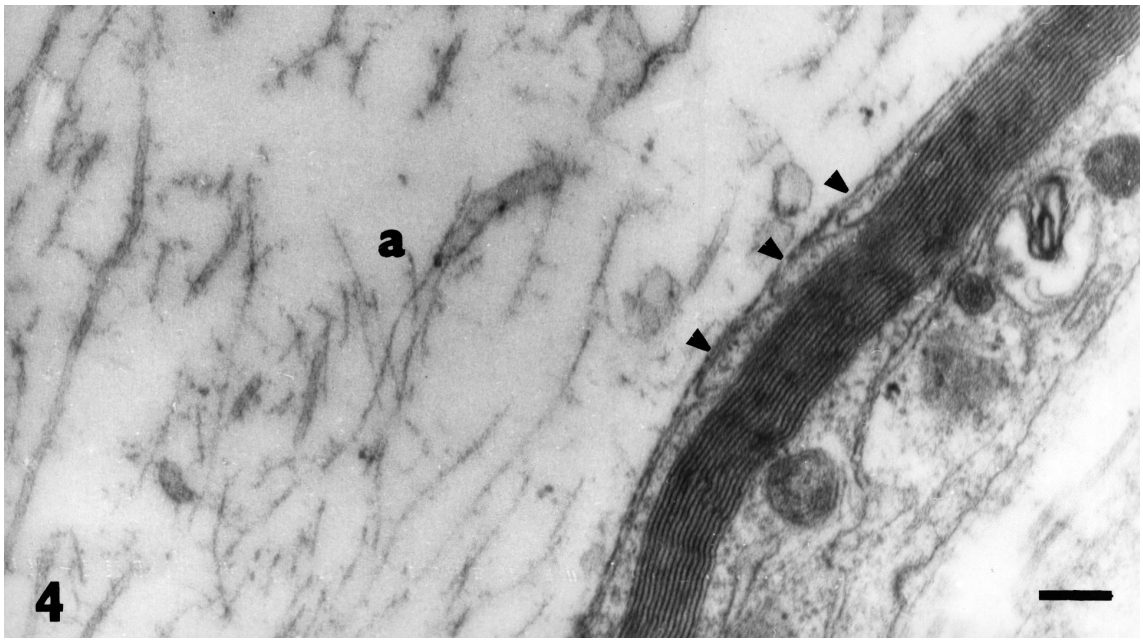

Fig. 4 The same fiber as shown on the fig. 1 - internodal region. Three terminal loops (marked by arrowheads) are found on inner surface of myelin sheath directing along the axon towards the Ranvier node. Bar, 0.2 μm.

Fig. 5 Paranodal region of myelinated nerve fiber at the 6th week of postnatal life. Terminal loops contact the axon approximately in the same surface area. They are all connected with the axon by axoglial junction so that the periaxonal space is reduced in this region. Arrowhead shows distinct periaxonal space in the internodal region. Bar, 0.2 μm.

ed with the axon by axoglial junction were seen in the longitudinal sections of the myelinating nerve fibers very often. They were single or in groups, in various distance from the paranodal region (Fig. 4). At the end of the sixth week all terminal loops contacting the axon were connected with it by axoglial junction (Fig. 5).

DISCUSSION

The study of longitudinal sections of myelinating nerve fibers has shown changes in the terminal loops of developing myelin lamellae. These changes seem to be crucial in understanding the mechanism of myelin sheath formation and growth.

It is known that the myelin lamellae terminate in paranodal region by terminal loops being joined with the axolemma by special axoglial junction. Periaxonal space between the terminal loops and adjacent axolemma is reduced from 20 nm to 2 -3 nm (13).

At the beginning of myelinogenesis, terminal loops, i. e. young loops, differ from the terminal loops in adult fiber. They are big and contact the axon in a large surface area. They are loosely applied to the axon, without being connected with the axolemma by axoglial junction. Periaxonal space is not reduced. Maturation of terminal loops results in changes of their shape, diminishing their contact area with the axon, periaxonal space reduction and in formation of the axoglial junction.

Gradual maturation of the terminal loops seems to be very important. In myelinating nerve fibres terminal loops of outer lamellae were more similar to the loops in an adult fiber, whereas the terminal loops of inner lamellae preserved the characteristics of young loops. This indicates, that terminal loops of outer lamellae are more mature than terminal loops of inner lamellae, outer lamellae are older than inner ones.We may draw conclusion that new myelin lamellae develop on the myelin sheath inner surface, i. e. the myelin spiral grows by elongation of inner mesaxon. This hypothesis is also supported by the finding of immature terminal loops distant from the paranodal region.

Longitudinal sections have a great advantage over the transverse sections (including the serial ones) showing better the changes occuring within one internode. Besides, longitudinal sections revealed something that can hardly be noticed in the transverse sections – the development of the axoglial junction. Webster did not mention it, probably he could not observe it.

Axoglial junction is a constant part of the myelin sheath in adult intact fiber in the peripheral as well as in the central nervous system (14,15,16). We consider the formation of axoglial junction as a main sign of the maturing terminal loops. Terminal loops of inner lamellae were immature during the whole period of the myelin sheath growth, their axoglial junction was absent. This finding has persuaded us that the myelin sheath inner lamellae are always the youngest.

Webster has focused on the study of mesaxons position. In the initial stages of myelinogenesis he observed changes in position of the inner end of mesaxon. The position of outer end of mesaxon remained relatively fixed. In more numerous lamellae formed, the position of inner and outer mesaxons was not so clear. Webster describes spiral movement of the outer mesaxon and the nucleus. He also suggests the spiral movement of the inner mesaxon and whole myelin coat in the opposite direction. His findings indicate that at the beginning of myelin sheath formation, lamella arises by elongation of the inner mesaxon. The problem of further increase of myelin lamella was concluded by him as „remaining poorly understood“. He suggests that the mesaxons, the incisures, and the sheath's outer and inner layers are large enough interfaces for the addition of the new membrane material at the rate required for the sheath's growth.

Examination of longitudinal sections shows no evidence of the outer mesaxon growth. Our findings have confirmed Webster's statement that within one internode the process of myelination is more advanced in the perinuclear region than close to the Ranvier nodes. Webster supported his statement with the incidence of larger number of myelin lamellae in the perinuclear region seen in serial transverse sections. In the longitudinal sections, we have also found more numerous lamellae in the perinuclear region. Another evidence supporting the hypothesis that the process starts in the centre of the internode and proceeds towards its ends, is for us a find-

ing of young, big terminal loops directed along the axon towards the Ranvier node. We observed such loops only at the inner surface of the myelin sheath. This makes us to suppose that these loops belong to the youngest lamellae. Absence of terminal loops directing towards the Ranvier node at the myelin sheath outer surface presents for us an evidence that the outer mesaxon does not substantially contribute to the increase of new myelin lamellae.

The study of myelinating nerve fibers in longitudinal sections made it possible for us to follow gradual maturation of the terminal loops and made us suppose that the myelin membrane formation is the result of inner mesaxon growth. Correlation of the longitudinal and transverse sections helped us to achieve a more complete conception of the myelinating nerve fiber than the transverse sections by themselves. In addition, longitudinal sections in the developing peripheral nerve enabled us to follow the structure differentiation in the Ranvier node which cannot be seen in the transverse sections without being correlated with the longitudinal sections (not documented). Therefore we believe that a careful ultrastructure analysis of myelinating nerve fibers seen in transverse and longitudinal sections can help to understand the myelin sheath development in more details.

REFERENCES

1. Geren BB. The formation from the Schwann cell surface of myelin in the peripheral nerves of chick embryos. Exp Cell Res 1954 7: 558-562.
2. Gamble HJ, Breathnach AS. An electron-microscope study of human foetal peripheral nerves. J Anat 1965 99, 3: 573-584.
3. Ochoa J. The sural nerve of the human foetus: electron microscope observations and counts of axons. J Anat 1971 108: 231-245.
4. Schroder JM, Bohl J, Brodda K. Changes of the ratio between myelin thickness and axon diameter in the human developing sural nerve. Acta Neuropathol 1978 43: 169-178.
5. Privat A. Morphological aspects of myelination. In: Neurological mutations affecting myelination. INSERM symposium No. 14, Elsevier, North Holland Biomedical Press 1980 p. 71-72.
6. Berthold CH, Mellstrom A. Postnatal development of node-paranode regions in two hind limb nerves of the cat. Develop Biol 1981 86: 111-116.
7. Saxod R, Bouvet J. Quantitative analysis of growth and myelination of cutaneous nerve fibers in the chick. Dev Neurosci 1982 5: 143-155.
8. Raine CS. Morphology of myelin and myelination. In: Morel P. editor. Myelin. New York: Plenum Press 1984 1-50.
9. Webster HdeF. The geometry of peripheral myelin sheaths during their formation and growth in rat sciatic nerve. J Cell Biol 1971 48: p. 348-367.
10. Webster HdeF. Development of peripheral myelinated and unmyelinated nerve fibres. In: Dyck PS, Thomas PK, Lambert E, editors. Peripheral Neuropathy. Philadelphia: Saunders Co. 1975 p. 37-61.
11. Friede RL. Control of myelin formation by axon caliber (With a model of the control mechanism). J comp Neurol 1972 144: 233-352.
12. Bunge MB, Bunge RP, Carey DJ, Cornbroocks CJ, Eldridge ChF, Williams AK, Wood PM. Axonal and nonaxonal influence on Schwann cell development. In: Developing and regenerating vertebrate nervous systems. Coates PV, Markwald RR, Kennedy AD, editors. Alan R. Liss, New York 1983 p. 71-105.
13. Landon DN, Hall S. The myelinated nerve fiber. In: Landon DM, Chapman GB, Hall S, editors. The peripheral nerve. London 1976 p. 1-105.
14. Rosenbluth J. Freeze-fracture studies of nerve fibres: evidence that regional differentiation of the axolemma depends upon glial contact. In: Aguayo AJ, editor. Current topics in nerve and muscle research. Amsterdam: Excerpta Medica. 1979 p. 200-206.
15. Hirano A. Structure of normal central myelinated fibres. In: Demyelinating disease: Basic and clinical electrophysiology. Waxman SG, Ritchie JM, editors. New York: Raven Press. 1981 p. 51-67.
16. Ishise J, Rosenbluth J. Nodal and paranodal structure during Wallerian degeneration in frog spinal nerve. Brain Res 1987 418: 85-97.

Received: June, 29, 2002
Accepted: September, 23, 2002

THE DISTRIBUTION PATTERN OF REDUCED NICOTINAMIDE ADENINE DINUCLEOTIDE PHOSPHATE DIAPHORASE EXHIBITING AND NITRIC OXIDE SYNTHASE IMMUNOREACTIVE NEURONS IN THE MIDBRAIN OF THE DOG

JOZEF MARŠALA[1], NADEŽDA LUKÁČOVÁ[1], KAROLÍNA KUCHÁROVÁ[1], DÁŠA ČÍŽKOVÁ[1], MARTIN MARŠALA[2]

[1]Institute of Neurobiology, Slovak Academy of Sciences, Košice, Slovak Republic
[2]Anesthesiology Research Laboratory, University of California, San Diego, CA, U.S.A.

Abstract

In this study we investigated the occurrence and regional distribution of nitric oxide synthesizing neurons in the midbrain of the dog using NADPH diaphorase histochemistry and nitric oxide synthase immunocytochemistry. While small NADPHd-exhibiting neurons were detected in the superficial layers of the superior colliculus and in the dorsolateral part of the periaqueductal gray, middle-sized and large NOS-immunoreactive neurons were found in the fifth and sixth layers of the superior colliculus and in the tegmental pedunculopontine nucleus. Pleomorphic population of NADPHd-exhibiting and/or NOS-immunoreactive neurons was found in the cuneiform and subcuneiform nuclei. NOS-immunoreactive neurons occurring in the Edinger-Westphal nucleus permitted to classify this nucleus as a nitric oxide synthesizing cranial portion of the parasympathetic system.

Key words: nitric oxide synthase, neurons, midbrain, Edinger-Westphal nucleus, dog

INTRODUCTION

Previous histochemical and immunocytochemical studies have suggested that reduced nicotinamide adenine dinucleotide phosphate diaphorase (NADPHd) and/or nitric oxide synthase (NOS) exist in distinct subsets of neurons occurring in many regions of the brain and spinal cord (1-5). It should be noted in this connection, that NADPHd-exhibiting and NOS-immunoreactive neurons are not exclusively associated with any particular neuromodulator or neurotransmitter, mainly, in some brainstem nuclei (6). Previous investigations from our laboratory have documented that many nitric oxide (NO) synthesizing neurons are localized at certain loci all along the rostrocaudal axis of the spinal cord in the dog and rabbit (7-11). Concurrently, high axonal NOS immunoreactivity (NOS-IR) and intense NADPHd staining was noted in all white matter columns, mainly in the ventral column and in the ventral part of the lateral column. It was experimentally confirmed, that distinct population of axonal NOS-immunopositivity is, in fact the bulbospinal respiratory nitric oxide synthase immunoreactive pathway clearly identified at high cervical level and ending in the phrenic nucleus of C3-C5 segments in the dog (12). However, the comparison of the extent of the bulbospinal respiratory NOS-immunoreactive pathway identified at upper cervical level with the cross-sectional area occupied by other (i.e. non-respiratory) NOS-immunoreactive axons suggests that a noticeable amount of nitrergic axons localized in the ventral and lateral columns might originate from the brain stem regions containing putative NOS-immunoreactive neurons. As a step towards understanding the origin of the descending NOS-immunoreactive pathways of brain stem origin a precise mapping of NOS-IR somata occurring in the midbrain and pontobulbar regions appeared as an undispensable tool. The aim of the present study was (i) to localize NOS-IR neurons in the tectal and tegmental regions of the midbrain and, (ii) to characterize neuronal NOS-IR cell types.

Address for correspondence:
Prof. Jozef Maršala, M.D., D.Sc., Institute of Neurobiology
Slovak Academy of Sciences
Šoltésovej 4
040 01 Košice
Slovak Republic

Phone: ++421 55 6785 062
Fax: ++421 55 6785 074
e-mail: marsala@saske.sk

METHODS

A total of 6 adult mongrel dogs of both sexes weighing 7-12 kg were used in this study. The dogs were divided into two groups. In the first group (n=3) the distribution of nitric oxide synthase-immunoreactive neurons in the midbrain and, in the second group (n=3) the occurrence of NADPH-exhibiting neurons in the brainstem in general and, in the tectal and tegmental regions of the midbrain in particular, were studied.

Nitric oxide synthase immunocytochemistry

The dogs (n=3) were anesthetized with a mixture of ketamin and xylazin (100 and 15 mg/kg body weight i.m.) and artificially ventilated in a respirator with oxygen and nitrous oxide (Anemat N8 Chirana). Afterward the animals were intracardially perfused with heparinized saline and subsequently with freshly prepared 4% paraformaldehyde in 0.1 M phosphate-buffered saline (PBS, pH 7.4). The brainstem was removed *in toto* and postfixed in the same fixative for an addinional 12 h. The following day the brain stem was cryoprotected in PBS containing graded sucrose (15-30%). Transverse sections (24 μm thick) were cut from the brainstem and arranged in an ascending order beginning at the pontomedullar transition up to the rostral portion of the midbrain. All sections were examined for neuronal nitric oxide synthase immunocytochemistry (13). The details of the tissue and section processing for NOS immunoreactivity are given elsewhere (12).

NADPH diaphorase histochemistry

For NADPHd histochemistry, the animals (n=3) were deeply anesthetized with pentobarbital (50 mg/kg, iv.) and perfused transcardially with saline followed by freshly prepared 4% paraformaldehyde +0.1% glutaraldehyde buffered with 1 M sodium phosphate, pH 7.4 . After perfusion fixation, the brain stem was carefully dissected out and stored *in toto* in the same fixative for 3-4 h. After postfixation, the brainstem was cryoprotected in an ascending concentration of sucrose (15-30%) with the same phosphate buffer and stored overnight at 4°C. Then, frozen transverse sections (42 μm thick) were cut from all specimens and processed for NADPH diaphorase activity using a modified histochemical procedure (14). Details of the processing are given elsewhere (12). It should be noted that no signs of a modified NADPH diaphorase histochemical staining or nitric oxide synthase immunoprocessing could be detected using different anaesthesia for two groups of experimental animals.

RESULTS

Morphologically heterogeneous populations of NADPHd-exhibiting and/or NOS-immunoreactive neurons have been identified in the tectal and tegmental portions of the midbrain. However, the pattern of distribution varies greatly in both compartments studied, similarly as it does in other brain regions. High number of small to medium size (20-40 μm in diameter) NADPHd-exhibiting neurons with two or three fine processes were observed in four superficial layers of the superior colliculus and in the dorsolateral part of the periaqueductal gray (Fig. 1A, 1D, 2A); the latter location corresponds with the griseum centrale mesencephali, subnucleus lateralis. Moreover, in the extent of layer III and IV distinct accumulation of heavily NADPHd-stained terminal fields, considered to be homotopic with so-called „glomeruli“ were observed and accompanied by light tissue bands containing loosely arranged fusiform intensely NADPHd-stained neurons.

The characteristic feature of the fifth and sixth layers of the superior colliculus is the presence of scattered middle-sized and large, plump, multipolar heavily NADPHd-stained and/or NOS-immunoreactive neurons possessing long dendrites (Fig. 1B, 2B, 2C). It should be noted that the sixth layer contains also large NOS-immunonegative neurons of the same size and they could be seen in the same row as NOS-IR somata. Both types of these large tectal neurons may be the source of origin for the tectospinal pathway. Pleomorphic population of variously stained NADPHd-exhibiting and/or NOS-IR neurons was found in the tegmental part of the midbrain. While fusiform or elongated NADPHd-stained and/or NOS-IR somata tend to prevail in the cune-

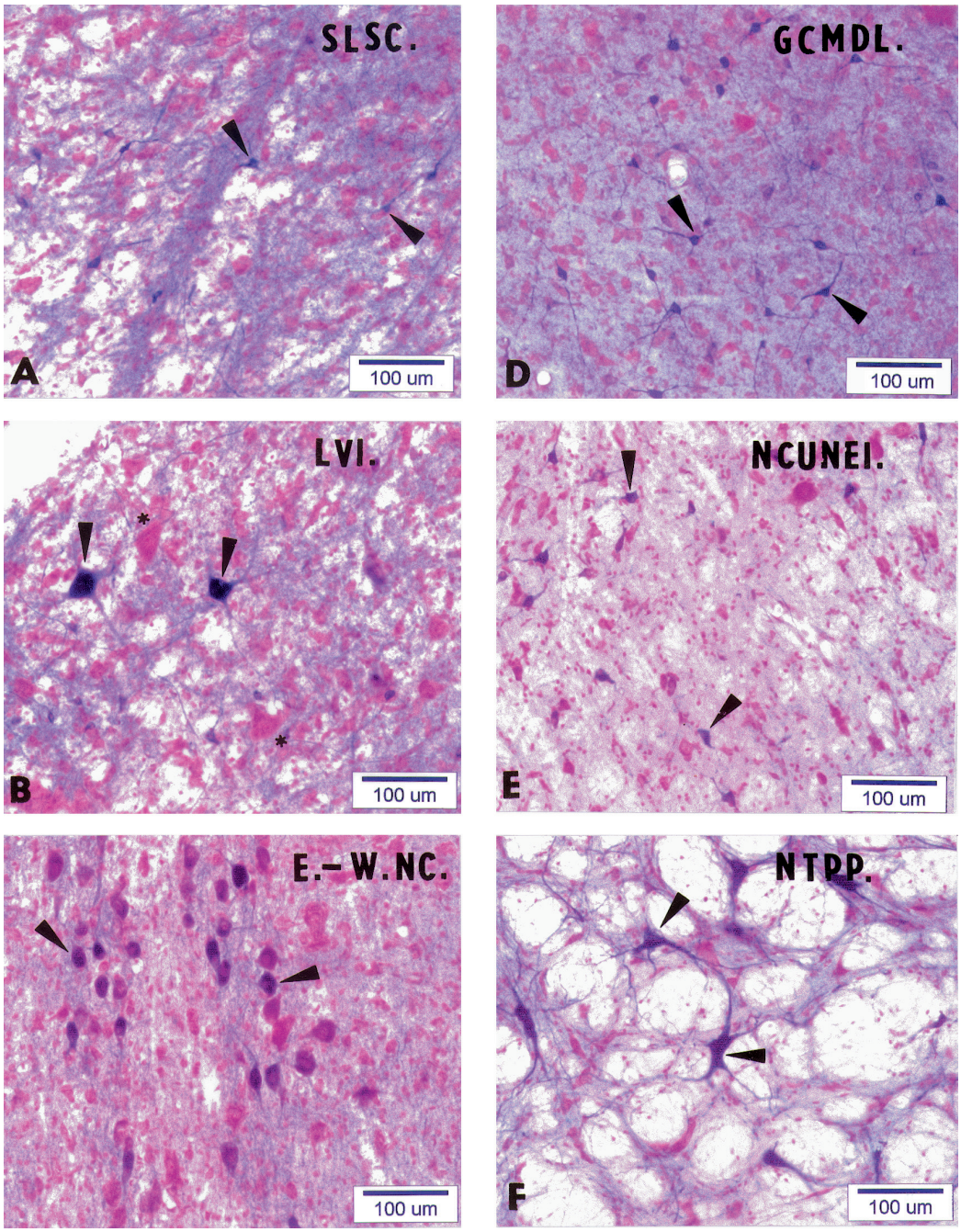

Fig.1. Microphotographs taken from the tectal and tegmental regions of the midbrain depicting various types of NADPHd-exhibiting neurons. A-arrowheads point to small NADPHd-exhibiting neurons in the superficial layers of the superior colliculus (SLSC); B-large, multipolar NADPHd-exhibiting neurons (arrowheads) can be seen in the sixth layer (LVI) of the superior colliculus; C-small, round or slightly elongated NADPHd-exhibiting neurons (arrowheads) are seen in the Edinger-Westphal nucleus (E.-W.NC.); D-small, round or spindle-shaped NADPHd-exhibiting neurons (arrowheads) are seen in the griseum centrale mesencephali, dorsolateral part (GCMDL.); E-dispersed, heavily NADPHd-stained neurons (arrowheads) were found in the cuneiform nucleus (NCUNEI.); F-large NADPHd-exhibiting somata (arrowheads) are characteristic for tegmental pedunculopontine nucleus (NTPP.).

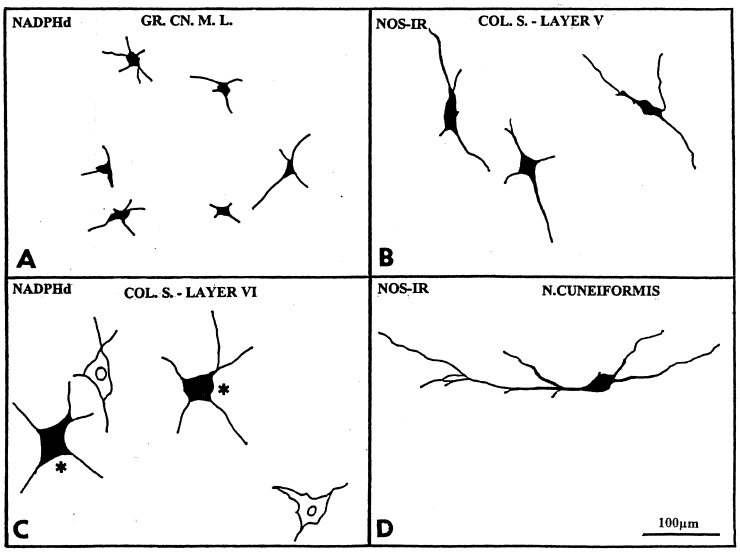

Fig.2. Camera lucida drawings of NADPHd-exhibiting and/or NOS-immunoreactive neurons. A-in the griseum centrale mesencephali, dorsolateral part (GR.CN.M.L.); B-fifth layer of the superior colliculus (COL.S.LAYER V); C-sixth layer of the superior colliculus (COL.S.LAYER VI) among large NADPHd-exhibiting neurons (asterisks) similar NADPHd-negative neurons are seen; D-fusiform type of NOS-immunoreactive neurons was found in the cuneiform nucleus (N.CUNEIFORMIS).

iform and subcuneiform nuclei (Fig. 1E, 2D), those identified in the nucleus tegmenti pedunculopontinus, subnucleus dissipatus and compactus, could be classified mostly as large, multipolar heavily stained neurons resembling at least in some loci to the large reticular NADPHd-exhibiting somata often seen in the pontine reticular formation (Fig. 1F).

Bilateral columns of round to oval (25-30 μm in diameter) heavily NADPHd-positive neurons have been disclosed in the tegmental part of the midbrain located just ventral to the aqueduct (Fig. 1C). Considering the position of both cell columns between the left and right magnocellular oculomotor nucleus, then the cell size and shape seen homogeneously all along the neuronal cell columns it becomes obvious that these highly NADPHd-positive neurons represent the parasympathetic Edinger-Westphall nucleus forming the parvocellular component of the oculomotor complex.

DISCUSSION

One of the most important findings of the present study is the detection of large, multipolar heavily NADPHd-positive and/or NOS-immunoreactive neurons dispersed among many NOS-immunonegative somata in the fifth and sixth layers of the superior colliculus. Their characteristic location is consistent with the occurrence of the neurons giving origin to the tectospinal pathway. It is therefore suggested, that the axons of the tectospinal pathway originating from middle-sized and large neurons in the deep layers of the superior colliculus descending after crossing in the dorsal tegmental decussation and terminating in the cervical spinal cord may be either NOS-immunoreactive or NOS-immunonegative fibers. Moreover, as was shown by recent degenerative and tract tracing studies the fibers of the tectospinal tract terminate chiefly in Rexeds lamina VII and VI, while some end in lamina VIII through which they enter (15-20).

The involment of other mesencephalic NADPHd-exhibiting and/or NOS-immunoreactive neurons in the formation of long descending nitrergic pathways mainly those described above in connection with the cuneiform, subcuneiform and tegmental pedunculopontine nuclei is highly probable, but as yet experimentally unsettled. On the other hand an unequivocal evidence presented above and describing the existence of the parasympathetic Edinger-Westphal nucleus located in close vicinity, i.e., rostral and dorsal to the right and left somatic magnocellular oculomotor nucleus demonstrates, for the first time, nitrergic nature of this parvocellular autonomous nucleus of the oculomotor nerve. It is well documented that axons emerging from the Edinger-Westphal nucleus proceed uncrossed, traverse the ciliary ganglion as its preganglionic fibers. Detailed analysis of these parasympathetic fibers in monkeys indicates that 96 per cent of preganglionic axons is for the innervation of the ciliary muscle and only 3 or 4 per cent for the

sphincter pupillae (21). Our histochemical and immunocytochemical analysis clearly documented the presence of the neuronal nitric oxide synthase in the neurons of the Edinger-Westphal nucleus, a finding permitting to classify this preganglionic pathway as a hitherto unknown thin NOS-immunoreactive parasympathetic bundle connecting the Edinger-Westphal nucleus and the above mentioned intraocular muscles. More interestingly, NOS-immunoreactive neurons of the Edinger-Westphal nucleus forming functionally an important component of the cranial portion of the parasympathetic system clearly differ from neurons of the sacral portion of the parasympathetic system containing mostly NOS-immunonegative neurons (8,22).

Acknowledgements:

The authors thank Mr. D. Krokavec, Ms. M. Špontáková, Mrs. M. Vargová and Mrs. I. Vrábelová for their excellent technical assistance.

The experimental work was supported by the VEGA Grants No. 2/7222/20, 2/1064/21 and 2/2079/22 from the SAS and by NIH grants NS 32794 and NS 40386 to M.M.

REFERENCES

1. Valtschanoff JG, Weinberg RJ, Rustioni A. NADPH diaphorase in the spinal cord of rats. J comp Neurol 1992; 321:209-227.
2. Dun NJ, Dun SL, Wu SY, Forstermann U, Schmidt HH, Tseng LF. Nitric oxide synthase immunoreactivity in the rat, mouse, cat and squirrel monkey spinal cord. Neuroscience 1993; 54:845-857.
3. Terenghi G, Riveros-Moreno V, Hudson LD, Ibrahim NB, Polak JM. Immunohistochemistry of nitric oxide synthase demonstrates immunoreactive neurons in spinal cord and dorsal root ganglia of man and rat. J Neurol Sci 1993; 118: 34-37.
4. Saito S, Kidd GJ, Trapp BD, Dawson TM, Bredt DS, Wilson DA, Traystman RJ, Snyder SH, Hanley DF. Rat spinal cord neurons contain nitric oxide synthase. Neuroscience 1994; 59: 447-456.
5. Lukáčová N, Čížková D, Maršala M, Jalč P, Maršala J. Segmental and laminar distributions of nicotinamide adenine dinucleotide phosphate-diaphorase-expressing and neuronal nitric oxide synthase-immunoreactive neurons versus radioassay detection of catalytic nitric oxide synthase activity in the rabbit spinal cord. Neuroscience 1994; 94: 229-237.
6. Mizukawa K, Vincent SR, McGeer PL, McGeer EG.. Distribution of reduced-nicotinamide-adenine-dinucleotide-phosphate diaphorase-positive cells and fibers in the cat central nervous system. J comp Neurol 1989; 279: 281-311.
7. Maršala J, Kluchová D, Maršala M. Spinal cord gray matter layers rich in NADPH diaphorase-positive neurons are refractory to ischemia-reperfusion-induced injury: a histochemical and silver impregnation study in rabbit. Exp Neurol 1997; 145: 165-179.
8. Maršala J, Vanický I, Maršala M, Jalč P, Orendáčová J, Taira Y. Reduced nicotinamide adenine dinucleotide phosphate diaphorase in the spinal cord of dogs. Neuroscience 1998; 85: 847-862.
9. Maršala J, Maršala M, Vanický I, Taira Y. Localization of NADPHd-exhibiting neurons in the spinal cord of the rabbit. J comp Neurol 1999; 406: 263-284.
10. Maršala J, Jalč P. Short-term changes of NADPH diaphorase-exhibiting neuronal pools in the spinal cord of rabbit after repeated sublethal ischemia. Physiol Res 2000; 49: 157-165.
11. Orendáčová J, Maršala M, Šulla I, Kafka J, Jalč P, Čízková D, Taira Y, Maršala J. Incipient cauda equina syndrome as a model of somatovisceral pain in dogs: spinal cord structures involved as revealed by the expression of c-fos and NADPH diaphorase activity. Neuroscience 2000; 95: 543-557.
12. Maršala J, Lukáčová N, Čížková D, Kafka J, Katsube N, Kuchárová K, Maršala M. The case for the bulbospinal respiratory nitric oxide synthase-immunoreactive pathway in the dog. Exp Neurol 2002; 177: in press.
13. Bredt DS, Hwang PM, Snyder SH. Localization of nitric oxide synthase indicating a neural role for nitric oxide. Nature 1990; 347:768-770.
14. Scherer-Singler U, Vincent SR, Kimura H, McGeer EG. Demonstration of a unique population of neurons with NADPH-diaphorase histochemistry. J Neurosci Methods 1983; 9: 229-234.
15. Papez JW, Freeman GL. Superior colliculi and their fiber connections in the rat. J comp Neurol 1930; 51: 409-439.
16. Rasmussen AT. Tractus tecto-spinalis in the cat. J comp Neurol 1936, 63: 501-526.
17. Tasiro S. Experimentell-anatomische Untersuchung über die efferenten Bahnen aus der Vierhügeln der Katze. Z mikr anat Forsch 1940; 47: 1-32.
18. Pearce GW, Glees P. The termination of the crossed tectospinal tract in the spinal cord of the cat. J Anat 1956; 90: 565-566.
19. Altman J, Carpenter MB. Fiber projections of the superior colliculus in the cat. J comp Neurol 1961; 116: 157-177.
20. Nyberg-Hansen R. The location and termination of tectospinal fibers in the cat. Exp Neurol 1964; 9: 212-227.
21. Warwick R. The ocular parasympathetic nerve supply and its mesencephalic sources. J Anat 1954; 88: 71-93.
22. Vizzard MA, Erickson K, de Groat WC. Localization of NADPH diaphorase in the thoracolumbar and sacrococcygeal spinal cord of the dog. J Auton Nerv Syst 1997; 64: 128-142.

Received: September, 16, 2002
Accepted: October, 20, 2002

STUDIES ON THE ROLE OF H_1 RECEPTORS IN ENDOGENOUS CENTRAL HISTAMINE-INDUCED ANTINOCICEPTIVE EFFECT IN RATS

JERZY JOCHEM, BARBARA RYBUS-KALINOWSKA, KRYSTYNA ŻWIRSKA-KORCZALA
Department of Physiology, Silesian Medical University, Zabrze, Poland

A b s t r a c t

Background and aim: Histamine belongs to central neurotransmitters which influence transmission of impulsation from nociceptors. Both exogenous histamine administered centrally and endogenous histamine, after blockage of its catabolism by histamine *N*-methyltransferase (HNMT) inhibitors, which leads to an increase in endogenous central histamine concentrations, produce an antinociceptive effect in many species. Previous studies demonstrate a dose-dependent analgesic effect of HNMT inhibitor SKF 91488 in tests inducing two kinds of noxious stimuli – thermal (tail-flick test) and mechanical (Randall-Selitto test) in rats. The aim of the present study was to examine the involvement of postsynaptic H_1 histamine receptors in SKF 91488-induced antinociceptive effect in rats.

Methods: Studies were performed in adult male Wistar rats treated intracerebroventricularly (*icv*) with SKF 91488 (100 μg) or saline (5 μl). To measure the involvement of H_1 receptors in SKF 91488-induced action, the rats were pretreated *icv* 30 min earlier with H_1 receptor antagonist chlorpheniramine (200 nmol). The antinociceptive activity was quantified using tail-flick test and paw pressure test (Randall-Selitto test) before treatment and at 15, 30, 45, 60 and 120 min after the administration of SKF 91488 or saline. In separate groups of chlorpheniramine-pretreated and saline-pretreated animals, central histamine concentrations were measured immunoenzymatically 15 min after SKF 91488 injection.

Results: SKF 91488 produced an analgesic effect both in tail-flick test and paw pressure test, which was measured at 15, 30, 45 and 60 min after treatment. Pretreatment with chlorpheniramine significantly inhibited SKF 91488-induced action in both tests, despite the fact that there were no differences in central histamine concentrations in the cerebral cortex (1.04 ± 0.12 *vs.* 1.1 ± 0.14 nmol/g), hypothalamus (5.54 ± 0.72 *vs.* 5.66 ± 0.81 nmol/g) and medulla oblongata (0.59 ± 0.13 *vs.* 0.63 ± 0.16 nmol/g) in comparison to saline-pretreated group. Chlorpheniramine (200, 300 nmol *icv*) given alone had no effect on pain perception.

Conclusions: The study demonstrates that SKF 91488 given *icv* evokes an antinociceptive effect, and thus confirms that it is an effective *in vivo* inhibitor of HNMT activity. Moreover, it is shown that H_1 histamine receptors are involved in SKF 91488 action in rats.

K e y w o r d s: endogenous histamine, pain perception, SKF 91488, chlorpheniramine, H_1 receptors, rat

INTRODUCTION

The histaminergic system influences various activities of the central nervous system, such as arousal mechanisms, fluid balance, food intake, temperature regulation, cardiovascular regulation, learning and pain perception (1, 2). The histaminergic neurones are concentrated mainly in the tuberomammillary nucleus of the posterior hypothalamus and send innervation, *via* ascending and descending fibres, to almost all parts of the brain, and thus may, as postulated, regulate the activity of the whole brain (3). Especially, the activation of the histaminergic system is characteristic of the response to the action of stimuli which may disturb integrity and homeostasis, including nociceptive stimuli (1, 4).

There is increasing evidence that the histaminergic system may directly influence the transmission of information from nociceptors (1, 3). Exogenous histamine administered into the brain lateral ventricle (*icv*) (5), the dorsal raphe nucleus or in the periaqueductal gray region in rats (6) evokes a dose-related antinociceptive action. Similar effects of endogenous histamine are observed after inhibition of histamine *N*-methyltransferase (HNMT) activity - the enzyme which catabolises histamine released from neurones. HNMT inhibitors, such as metoprine (7), BW 301U (8) and SKF 91488 (8), produce an increase in central histamine concentrations and are generally accepted in studies on the biological role of the histaminergic system.

A d d r e s s f o r c o r r e s p o n d e n c e:
Dr n. med. Jerzy Jochem, Katedra i Zakład Fizjologii, Śląska Akademia Medyczna, ul. H. Jordana 19, 41-808 Zabrze, Poland
Phone/fax: ++48 32 272 23 62
e-mail: jjochem@poczta. pl

In addition to pharmacological methods used for the histaminergic system activation, studies by Philippu *et al.* clearly demonstrate the increase in synthesis and/or release of endogenous central histamine in stress conditions (9). Our previous results show that restraint immobilisation stress potentiates the antinociceptive effect induced by SKF 91488 in rats, despite the fact that it does not influence endogenous central histamine concentrations (10). Thus, our findings may confirm the activation of the histaminergic system in conditions of immobilisation stress in rats, which also influences the transmission of impulsation from nociceptors.

The present paper, being a continuation of our previous studies on the role of the histaminergic system in modulation of pain transmission, demonstrates the involvement of H_1 histamine receptors in HNMT inhibitor SKF-91488-induced antinociceptive effect in rats.

METHODS

Male Wistar rats weighing 230-250 g (5-6 months old) were used in all experiments. The animals were housed five per cage, under controlled conditions of temperature (20-22°C), humidity (60-70%), lighting (12 h light/dark cycle) and provided with food and water *ad libitum*. All procedures were carried out according to EU directives and reviewed by Ethics Committee of the Medical University of Silesia.

For *icv* treatment rats were prepared 5-7 days before the experiment by stereotaxic implantation, under ketamine/xylazine (60 mg/kg + 10 mg/kg intraperitoneally) anaesthesia, of polyethylene cannula into the right brain lateral ventricle as described previously (4). All *icv* injections were given in 5.0 µl of saline vehicle.

The antinociceptive activity was quantified using tail-flick test (11) and paw pressure test (Randall-Selitto test) (12). In the tail-flick test, the thermal stimulus from analgesymeter (Porfex, Białystok, Poland) was adjusted in preliminary studies to produce a tail-flick response in control rats within 4-6 s. Animals with higher control values were excluded. A cut-off time of 15 s was used to avoid blistering. Three tail-flick latencies, at 60 s intervals, were taken and the mean value was recorded. Paw pressure thresholds (Randall-Selitto test) were determined for the left hind paw of rats using an automated analgesymeter (Ugo Basile Biological Research Apparatus, Comerio – Varese, Italy). Rats scoring below 50 g or over 70 g before treatment were rejected. An arbitrary cut-off value of 200 g was adopted.

The rats were *icv* treated with SKF 91488 (100 µg) or saline (5 µl). Since SKF 91488 (4-[N,N-dimethylamino]butylisothiourea dihydrochloride) does not cross the blood-brain barrier, similarly to the previous studies (10, 13), it was administered centrally. In order to measure the involvement of H_1 histamine receptors in SKF 91488-induced action, the animals were pretreated *icv* 30 min earlier with H_1 receptor antagonist chlorpheniramine (200 nmol). The antinociceptive activities were measured before treatment and at 15, 30, 45, 60 and 120 min after *icv* administration of SKF 91488 or saline. All the experiments were performed between 8.00 and 12.00 am.

In chlorpheniramine-pretraeted and saline-pretreated animals (n = 5), endogenous central histamine concentrations were measured 15 min after SKF 91488 injections, since at that time the antinociceptive activities were most pronounced. Briefly, after decapitation of rats, the brains were rapidly removed and the cerebral cortex, hypothalamus and medulla oblongata were quickly dissected on a glass plate chilled on ice, according to the procedure by Glowinski and Iversen (14). The samples were homogenised – the hypothalamus in 0.5 ml, the cerebral cortex and medulla oblongata in 10 volumes (w/v) of ice-cold 0.9% NaCl. After centrifugation, 100 µl of the supernatant was used for measurement of histamine concentration by commercially available enzyme immunoassay (Immunotech, France) without modifications. The sensitivity of the method was 0.2 nmol/l. The mean recovery of standard histamine was 91% (ranging from 86 to 112%).

The following drugs were used: SKF 91488, (±)-chlorpheniramine maleate, xylazine (Research Biochemicals Incorporated, USA), ketamine (Gedeon Richter, Hungary). All drug solutions were prepared fresh on the day of the experiment.

Table 1. Effects of chlorpheniramine and SKF 91488 on the pain threshold in the rat paw pressure test (Randall-Selitto test); 6 to 9 animals per group; initial threshold pressure 63.6 ± 4.8 g; * $p < 0.05$ *vs.* the pretreatment value; in chlorpheniramine-pretreated group # $p < 0.05$ *vs.* corresponding value in saline-pretreated group

Pre-treatment (*icv*)	Treatment (*icv*)	Pressure (g)				
		Time after *icv* treatment				
		15 min	30 min	45 min	60 min	120 min
Saline (5 µl)	Saline (5 µl)	59.4 ± 5.6	61.2 ± 5.2	62.3 ± 4.3	60.4 ± 5.9	63.5 ± 3.9
Saline (5 µl)	SKF 91488 (100 µg)	157.3 ± 6.8*	138.2 ± 9.4*	117.1 ± 8.1*	88.3 ± 7.4*	59.1 ± 5.4
Chlorpheniramine (200 nmol)	Saline (5 µl)	61.7 ± 5.3	58.4 ± 5.6	61.3 ± 4.5	64.5 ± 5.7	62.4 ± 6.6
Chlorpheniramine (300 nmol)	Saline (5 µl)	63.3 ± 5.1	61.9 ± 3.3	59.7 ± 6.3	58.7 ± 4.8	58.1 ± 6.7
Chlorpheniramine (200 nmol)	SKF 91488 (100 µg)	98.4 ± 6.6*#	87.5 ± 7.9*#	72.4 ± 4.9*#	61.4 ± 4.1#	59.4 ± 5.6

Table 2. Effects of chlorpheniramine and SKF 91488 on the pain threshold in the rat tail-flick test; 6 to 9 animals per group; initial time latency 5.3 ± 0.4 s; * $p < 0.05$ *vs.* the pretreatment value; in chlorpheniramine-pretreated group # $p < 0.05$ *vs.* corresponding value in saline-pre-treated group

Pre-treatment (*icv*)	Treatment (*icv*)	Tail-flick response (s)				
		Time after *icv* treatment				
		15 min	30 min	45 min	60 min	120 min
Saline (5 µl)	Saline (5 µl)	5.2 ± 0.5	5.8 ± 0.9	4.8 ± 1.2	4.9 ± 0.9	5.7 ± 1.1
Saline (5 µl)	SKF 91488 (100 µg)	15.0 ± 0.0*	13.8 ± 0.9*	10.2 ± 1.3*	8.8 ± 1.4*	5.1 ± 1.5
Chlorpheniramine (200 nmol)	Saline (5 µl)	5.1 ± 0.4	5.5 ± 0.6	5.4 ± 0.9	5.6 ± 0.7	5.2 ± 0.6
Chlorpheniramine (300 nmol)	Saline (5 µl)	5.3 ± 0.5	5.1 ± 0.3	5.5 ± 0.3	4.9 ± 0.8	5.1 ± 0.6
Chlorpheniramine (200 nmol)	SKF 91488 (100 µg)	9.8 ± 1.9*#	7.5 ± 0.7*#	5.4 ± 0.4#	4.9 ± 0.5#	5.3 ± 0.4

All data are given as means ± standard deviation with $p < 0.05$ considered as the level of significance. Differences between groups were analysed using a one-way analysis of variance. Significance of differences within groups over time was tested with a Student's t-test.

RESULTS

There were no differences between the groups in initial nociceptive responses to thermal (tail-flick test) or mechanical (Randall-Selitto test) noxious stimuli, the values being 4.9 ± 0.5 s and 63. 4 ± 6.1 g, respectively. SKF 91488 (100 µg) produced an analgesic action in both tests, which

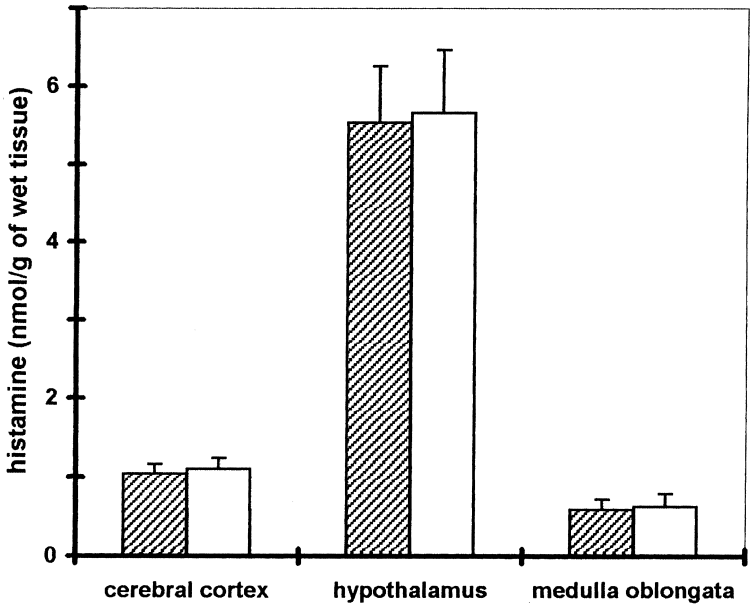

Fig. 1. Concentrations of histamine in the cerebral cortex, hypothalamus and medulla oblongata in rats pretreated with chlorpheniramine (200 nmol *icv*, ▨) and saline (5 µl *icv*, □), 15 min after SKF 91488 (100 µg *icv*) injection

was measured at 15, 30, 45 and 60 min after treatment, with a maximum effect at 15 min after injection (Table 1, 2).

Pre-treatment with histamine H_1 receptor antagonist chlorpheniramine (200 nmol *icv*) significantly inhibited the action of SKF 91488 in both tests, whereas chlorpheniramine (200, 300 nmol *icv*) given alone had no effect on pain perception (Table 1, 2).

There were no differences in endogenous central histamine concentrations between chlorpheniramine-pretreated and saline-pretreated animals 15 min after SKF 91488 (100 µg) injection in the cerebral cortex (1.04 ± 0.12 *vs.* 1.1 ± 0.14 nmol/g), hypothalamus (5.54 ± 0.72 *vs.* 5.66 ± 0.81 nmol/g) and medulla oblongata (0.59 ± 0.13 *vs.* 0.63 ± 0.16 nmol/g) – Fig. 1.

DISCUSSION

The present results confirm an analgesic action of endogenous histamine after inhibition of HNMT activity with SKF 91488. Moreover it is demonstrated that H_1 receptors are involved in endogenous histamine antinociceptive effect.

The histaminergic system is implicated in the central modulation of pain transmission, which has been demonstrated in many species (1, 2), however, much about its function remains to be investigated. Exogenous histamine administered *icv*, *via* H_1 and H_2 receptors, produces an antinociceptive effect, since pretreatment with both H_1 and H_2 antagonists has been reported to inhibit exogenous histamine-induced antinociception (5). Our previous (10) and present studies show that an increase in endogenous histamine concentrations after inhibition of HNMT activity with SKF 91488 also leads to an analgesic effect measured in tests using two different kinds of noxious stimuli: thermal (tail-flick test) and mechanical (Randall-Selitto test) in rats, however, the receptors involvement, in contrast to exogenous histamine, is not clear.

Studies of Braga *et al.* demonstrate that central histamine inhibits the evoked firing recorded from thalamic neurones, induced by peripheral algogenic stimuli in a rat model of arthritis (15). Interestingly, the inhibition by histamine is seen only on firing evoked by algogenic stimuli, but not on spontaneous firing (15). On the other hand, our previous studies demonstrate that the activation of the histaminergic system in rats subjected to restraint immobilisation stress potentiates SKF 91488-induced antinociceptive effect, although without additional influence on

the central histamine concentration (10). Both facts suggest the role of histamine in modulation of pain transmission upon activation of the histaminergic system.

Since the antinociceptive effect of histamine in the thalamus is antagonised by pre-treatment with H_1 receptor antagonist mepyramine, the H_1 receptors are involved in the inhibitory influence of histamine on evoked firing (16). Furthermore, studies by Malmberg-Aiello *et al.* demonstrate that activation of the central H_1 receptors increases sensitivity to noxious stimuli in rodents (17). Also the present study demonstrates the involvement of H_1 receptors in endogenous central histamine-induced analgesic action since chlorpheniramine inhibits SKF 91488 effect. In addition, the present study demonstrates increased, in comparison to saline-treated rats (10), concentrations of endogenous histamine in the cerebral cortex, hypothalamus and medulla oblongata in chlorpheniramine-pretreated and saline-pre-treated animals, with no differences between the two groups, which confirms the inhibition of an antinociceptive effect due to the blockage of H_1 receptors. On the other hand, since H_1 receptor blockage does not influence the pain threshold in the control saline-treated animals, the results suggest that endogenous histamine, acting *via* H_1 receptors, does not play the essential role in pain transmission in normal conditions.

Several lines of evidence have suggested the interactions between the histaminergic and the opioidergic systems, not only in regulation of pain transmission but also in the central cardiovascular control (18, 19). For example, histamine receptor antagonists microinjected into the periaqueductal gray attenuate morphine-induced antinociception in rats (20). Furthermore, studies by Suh *et al.* demonstrate the involvement of spinal H_1 receptors in antinociceptive effects of morphine and β-endorphin administered intrathecally (21). On the other hand, histamine produces opposite effects to endogenous opioides in the central cardiovascular regulation in haemorrhagic shock. Previous studies clearly demonstrate that there is an activation of opioid and non-opioid (histaminergic, cholecystokininergic, thyreoliberininergic) neuronal systems in severe disturbance of circulatory homeostasis, for example after a large blood loss (18, 19). Indeed, findings by Philippu *et al.* demonstrate that the decrease in blood pressure in cats is associated with the rise in the release of endogenous histamine from the posterior hypothalamus (9). Moreover, studies by Itoh *et al.* show the increase in the brain level of a predominant metabolite of brain histamine tele-methylhistamine, however, without changes in histamine concentrations, resulting from different kinds of stress, including the exposure to tail pinch in rats and tail pinch, placing on a hot plate or subjecting to acetic acid-induced writhing in mice (22). Therefore, histamine turnover is altered under stress conditions, which may lead to the mobilisation of compensatory mechanisms, including the increase in β-endorphin, ACTH and corticosterone secretion in stressed rats (1, 23). Previous studies from our laboratory demonstrate that in critical haemorrhagic hypotension both exogenous histamine administered *icv* (4, 24-26) and endogenous histamine, after inhibition of HNMT activity (27), produce a dose-dependent long lasting pressor effect accompanied by an increase in the survival ratio of 2 h. Interestingly, the pressor effects of histamine in rats subjected to critical haemorrhagic hypotension are a few fold higher compared to those in normotensive animals (4, 27), which demonstrates the important role of the histaminergic system in the maintenance of circulatory homeostasis in critical hypovolaemia. Thus, it can be suggested that interactions between the histaminergic and the opioidergic systems in the state of disturbed homeostasis may play an important role not only in the central modulation of pain transmission and cardiovascular regulation, but also in a reaction complex necessary to survive in stress conditions.

In conclusion, the present study confirms the role of the histaminergic system in pain perception mechanisms, demonstrating that H_1 receptors are involved in endogenous central histamine-induced antinociceptive effect in rats. On the other hand, it is shown that blockage of H_1 receptors does not influence the pain threshold in the control saline-treated animals, which suggest that the effect is observed after stimulation of the histaminergic system. This finding is in accordance with the hypothesis that the activation of the histaminergic system in the states of disturbed homeostasis may mobilise compensatory mechanisms, including inhibition of information transmission from nociceptors, which is essential for escape and survival.

REFERENCES

1. Brown RE, Stevens DR, Haas HL. The physiology of brain histamine. Progr Neurobiol 2001; 63: 637-672.
2. Schwartz J-C, Arrang J-M, Garbarg M, Pollard H, Ruat M. Histaminergic transmission in the mammalian brain. Physiol Rev 1991; 71: 1-51.
3. Wada H, Inagaki N, Yamatodani A, Watanabe T. Is the histaminergic neuron system a regulatory center for whole-brain activity? Trends Neurosci 1991; 14: 415-418.
4. Jochem J. Cardiovascular effects of histamine administered intracerebroventricularly in critical haemorrhagic hypotension in rats. J Physiol Pharmacol 2000; 51: 229-239.
5. Jochem J, Pogorzelska T. Influence of histamine H_1 and H_2 and opioid receptor antagonists on antinociceptive reaction after histamine administered intracerebroventricularly in rats. J Physiol Pharmacol 1996; 47 (Supplement 2): 36.
6. Glick SD, Crane LA. Opiate-like and abstinence-like effects of intracerebral histamine administration in rats. Nature 1978; 273: 547-549.
7. Malmberg-Aiello P, Lamberti C, Ghelardini C, Giotti A, Bartolini A. Role of histamine in rodent antinociception. Br J Pharmacol 1994; 111: 1269-1279.
8. Malmberg-Aiello P, Lamberti C, Ipponi A, Hänninen J, Ghelardini C, Bartolini A. Effects of two histamine-N-methyltransferase inhibitors, SKF 91488 and BW 301U, in rodent antinociception. Naunyn-Schmiedebergs Arch Pharmacol 1997; 355: 354-360.
9. Philippu A, Hagen R, Hanesch U, Waldmann U. Changes in the arterial blood pressure increase the release of endogenous histamine in the hypothalamus of anaesthetized cats. Naunyn-Schmiedebergs Arch Pharmacol 1983; 323: 162-167.
10. Jochem J, Rybus-Kalinowska B, Żwirska-Korczala K. Influence of restraint stress on endogenous central histamine-induced antinociceptive effect in rats: studies with histamine N-methyltransferase inhibitor SKF 91488. Acta Med Mart 2002; 2 (2): 3-8.
11. D'Amour FE, Smith DL. A method for determining loss of pain sensation. J Pharmacol Exp Ther 1941; 72: 74-79.
12. Randall LO, Selitto JJ. A method for measurement of analgesic activity of inflamed tissue. Archiv Int Pharmacodynamic 1957; 111: 409.
13. Jochem J, Żwirska-Korczala K, Rybus-Kalinowska B, Jagodzińska J, Korzonek-Szlacheta I. Influence of SKF 91488, histamine N-methyltransferase inhibitor, on the central cardiovascular regulation during controlled, stepwise hemorrhagic hypotension in rats. Pol J Pharmacol 2002; 54: 237-244.
14. Glowinski J, Iversen LL. Regional studies of catecholamines in the rat brain. I. The disposition of [^{3}H]norepinephrine, [^{3}H]dopamine and [^{3}H]dopa in various regions of the brain. J Neurochem 1966; 13: 655-669.
15. Braga PC, Sibilia V, Guidobono E, Pecile A, Netti C. Electrophysiological correlates for antinociceptive effects of histamine after intracerebral administration to the rat. Neuropharmacology 1992; 31: 937-941.
16. Braga PC, Soldavini E, Pecile A, Sibilia V, Netti C. Involvement of H_1 receptors in the central antinociceptive effect of histamine: pharmacological dissection by electrophysiological analysis. Experientia 1996; 52: 60-65.
17. Malmberg-Aiello P, Lamberti C, Ipponi A, Bartolini A, Schunack W. Evidence for hypernociception induction following histamine H_1 receptor activation in rodents. Life Sci 1998; 63: 463-476.
18. Bertolini A. The opioid/anti-opioid balance in shock: a new target for therapy in resuscitation. Resuscitation 1995; 30: 29-42.
19. Jochem J, Jośko J, Gwóźdź B. Endogenous opioid peptides in haemorrhagic shock - central cardiovascular regulation. Med Sci Monit 2001; 7: 545-549.
20. Barke KE, Hough LB. Simultaneous measurement of opiate-induced histamine release in the periaqueductal gray and opiate antinociception: an in vivo microdialysis study. J Pharmacol Exp Ther 1993; 266: 934-942.
21. Suh HW, Song DK, Choi YS, Kim YH. Effects of intrathecally injected histamine receptor antagonists on the antinociception induced by morphine, β-endorphin, and U50, 488H administered intrathecally in the mouse. Neuropeptides 1996; 30: 485-490.
22. Itoh Y, Oishi R, Nishibori M, Saeki K. Effects of nociceptive stimuli on brain histamine dynamics. Jpn J Pharmacol 1989; 49: 449-454.
23. Bugajski J, Gądek A. Central H_1- and H_2-histaminergic stimulation of pituitary-adrenocortical response under stress in rats. Neuroendocrinology 1983; 36: 424-430.
24. Jochem J. Haematological, blood gas and acid-base effects of central histamine-induced reversal of critical haemorrhagic hypotension in rats. J Physiol Pharmacol 2001; 52: 447-458.
25. Jochem J. Central histamine-induced reversal of critical haemorrhagic hypotension in rats - haemodynamic studies. J Physiol Pharmacol 2002; 53: 75-84.
26. Jochem J. Central histamine-induced reversal of haemorrhagic shock versus volume resuscitation in rats. Inflamm Res 2002; 51 (Supplement 1): S57-S58.
27. Jochem J. Endogenous central histamine-induced reversal of critical haemorrhagic hypotension in rats - studies with histamine N-methyltransferase inhibitor SKF 91488. Inflamm Res 2002, 51: 551-556.

Received: November, 29, 2002
Accepted: December,12, 2002

EFFECT OF CYTOSTATIC DRUGS ON THE ENDOTHELIUM AND PLATELETS

Viera Tomášková jr.[1], Eva Rozborilová[2], Emília Flochová[3], Ján Staško[3], Peter Kubisz[3]

[1]Department of Internal Medicine 1, Comenius University, Jessenius Faculty of Medicine, Martin, Slovak Republic
[2]Department of Pneumophthisiology and Respiratory Diseases, Comenius University, Jessenius Faculty of Medicine, Martin, Slovak Republic
[3]Department of Haematology and Blood Transfusion, Comenius University, Jessenius Faculty of Medicine, Martin, Slovak Republic

Abstract

The aim of the study was to investigate the effect of cytostatic therapy on the endothelium and platelets in haemato-oncological patients. The beta-thromboglobulin (BTG), platelet factor 4 (PF4), thrombospondin (TSP), von Willebrand factor (vWF), thrombomodulin (TM), fibronectin (FN), tissue plasminogen activator (tPA) and inhibitor of plasminogen activator 1 (PAI-1) plasma levels were measured during polychemotherapy (period of 6 months). Venous blood was taken before the initiation of polychemotherapy as well as before and after each course of cytostatic treatment. All parameters were quantified by Elisa in the plasma samples of 37 patients.

The BTG, PF4, vWF, TM and FN plasma levels were significantly elevated ($p<0.001$) and those of PAI-1 significantly decreased ($p<0.05$) in the patient group compared to the control group. Our results suggest that haematological malignancies affect the function of both platelets and endothelium already before the initiation of polychemotherapy.

Key words: haemostasis, endothelium, cytostatic therapy, platelets

INTRODUCTION

Changes in haemostasis are very frequent and variable in the case of oncological disease. These abnormalities may be enhanced by the intensive antitumour therapy. Malignant diseases themselves may affect the haemostatic system and its individual components (endothelium, platelets, plasma coagulation factors, fibrinolytic system) by various pathogenetic mechanisms (1).

Chemotherapy induces often the release of procoagulants or activators of fibrinolysis from disintegrated cells in the tumour (2). Cytostatic drugs by themselves may, however, induce the activation of various mechanisms and they affect not only the number of platelets, but also their function as well as the functions of endothelial cells. Increased platelet aggregation was observed after combined therapy with interferon gama and tumour necrosis factor alpha (3). Treatment with vincristine resulted in lower incidence of aggregation in animal models (4). High chemotherapeutical doses, e.g. treatment with carmustine, cyclophosphamide, is associated with platelet secretion defect (5). The pathogenesis of the toxic effect of chemotherapeutic drugs on the endothelial cells may also include several factors. Endothelium damage may be local, e.g. in the case of 5-fluorouracil utilised in ophtalmology (6), or generalised, e.g. after the treatment with a combination of cytostatic drugs containing mitomycine C, cis-platinum, bleomycin and vinblastine (7).

The imbalance in the fibrinolytic system is caused by several cytostatic drugs - streptozocin, azelaic acid, bleomycin, cycloheximide, actinomycin D and doxorubicin (8, 9, 10, 11, 12). A complex effect on haemostasis is exerted by steroids or L-asparaginase (13).

The objective of our study was to investigate the effect of cytostatic therapy on endothelium and platelets, i.e. to find out whether and by which mechanisms is haemostasis (particulary related to endothelium and platelets) affected by cytostatic therapy.

Address for correspondence:
Prof. Peter Kubisz, M.D., D.Sc., Department of Haematology and Blood Transfusion, Martin Faculty Hospital, Kollárova 2, 036 59 Martin, Slovak Republic
Phone: ++421 43 4203 233, ++421 43 4133 308
Fax: ++421 43 4132 061
e-mail: kubisz@jfmed.uniba.sk

METHODS

A total of 37 patients with recently diagnosed haemato-oncological disease were enrolled in this study after informed consent and in accordance with the ethical standards. Before entering the study patients were neither treated with cytostatic drugs nor exposed to the radiotherapy. The characteristics of the patient group with respect to the type of haemato-oncological disease and to the age and gender are shown in Table 1 and 2, respectively. The control group consisted of 38 healthy individuals.

The first cycle of polychemotherapy including 6 cytostatic treatments was determined as the follow-up period. Venous blood was taken 12 times: the first sample was taken before the beginning of polychemotherapy and the followed blood specimens were collected before and after each cytostatic treatment. Venous blood was obtained by the method of non-traumatic venous punction into the solution of 3,8% sodium citrate (the ratio blood to sodium citrate being 9:1). The plasma was separated by centrifugation for 10 min at 1500 rpm and it was stored at –20°C prior to the analysis. The levels of selected parameters (BTG, PF4, TSP, vWF, TM, FN, tPA and PAI-1) were measured by the commercial kits Asserachrom Elisa /Diagnostica Stago, France/.

The type and phase of haemato-oncological disease were in close relation with the specific combination of chemotherapeutic drugs and their dosage. A broad spectrum of cytostatic drugs has been used in the study: bleomycin, cyclophosphamide, cytosin-arabinoside, dacarbazine, dexamethasone, doxorubicin, etoposide, idarubicin, L-asparaginase, lomustine, melphalan, mercaptopurine, metothrexate, mitoxantrone, mustargen, prednisone, procarbazine, teniposide, vinblastine and vincristine.

Several statistical methods : chi-square, Kolmogorov-Smirnov, Wilcoxon, Kruskal-Wallis and Mann - Whitney tests were used for the processing of experimental results. The quantitative parameters were characterized by the median and the 95% confidence interval (CI). The level $p < 0.05$ was considered to be significant.

Table 1. Patient group and the type of haemato-oncological disease

Disease	Number of patients	Percentage (%)
Acute leukemia	8	21.6
Non-Hodgkin lymphoma	15	40.6
Hodgkin disease	12	32.4
Myeloma multiplex	2	5.4
Total	37	100.0

Table 2. Patient group according to the age and gender

	Age (y)	Age males (y)	Age females (y)
Group size	37	19	18
Median	49	55	46
95% CI	(13:86)	(21:86)	(13:74)
y-years CI-confidence interval			

RESULTS

There were no significant differences found in the patient group between the values of individual parameters in the 1st and 12th sampling. Correspondingly, no trends indicating neither increase nor decrease in the values of measured parameters were observed over the examined period in the patient group. The average values were determined for each of 8 parameters. We

Table 3. Platelet markers - median values and results of Mann-Whitney test

Parameter	Controls	Patients	Significance
BTG	22.5	123.4	p<0.001
PF4	3.7	45.1	p<0.001
TSP	18.3	18.5	NS
NS - no significant			

Table 4. Endothelial markers - median values and results of Mann-Whitney test

Endothelial markers			
Parameter	*Controls*	*Patients*	*Significance*
vWF	1.20	1.52	p<0.001
TM	38.6	51.0	p<0.001
PAI-1	27.9	13.4	p<0.05
TPA	8.2	7.4	NS
FN	304	456	p<0.001
NS - no significant			

tested the median and 95% CI for the values of individual parameters of all specimens (irrespective of time sequence) both in the patient and control groups. The medians of BTG, PF4, vWF, FN and TM plasma levels were significantly higher ($p < 0.001$) and the median those of PAI-1 significantly lower ($p < 0.05$) in the patient group compared to the control one. The results are depicted in Table 3 and Table 4.

DISCUSSION

The results indicate that the BTG, PF4, TM and FN plasma levels were significantly increased and those of the PAI-1 significantly reduced in the patient group. However, we may conclude, that these values were modified before the initiation of polychemotherapy. Our results confirm the reports about the effects of malignant disease processes on haemostasis (1).

Lane et al. declare that BTG is the most sensitive marker of platelet release reaction in vivo (14). The significant increase of BTG plasma levels was found in our patient group. Tumour cells are able to induce platelet activation (15, 16). The TSP levels are usually increased in parallel with increased BTG and PF4. It was probably a matter of assay sensitivity that we did not observe an increase of TSP levels. However, the increased levels of both BTG and PF4 indicated changes of platelet activity in our patient group already before the initiation of polychemotherapy.

The levels of endothelial markers in the blood are elevated when the endothelium is dysfunctional or damaged (17). To discriminate between these two conditions, the best results were obtained by combined estimation of vWF and TM (17). Alteration of the endothelium in our patient group was more pronounced as indicated by elevated levels of both vWF and TM ($p<0,001$). Shift in the equilibrium in favour of the procoagulant factors is supported also by a significant increase of FN level in patient group.

The majority of published information suggests that malignant cells produce PAI-1 and that tumour diseases are associated with the reduced fibrinolytic activity of blood in spite of the local increase in fibrinolysis (18). The reduced levels of PAI-1 were found in our patient group. This finding together with the normal levels of tPA, might indicate the higher fibrinolytic activity. As a matter of fact, degradation of fibrin and fibrinogen is associated also with different plasminogen – independent mechanisms (19). In our study, the balance between fibrinolytic and inhibitory systems was clearly disturbed even before the onset of polychemotherapy.

Our results suggest that endothelial and platelet functions were modified already before the

initiation of cytostatic therapy and this condition persisted during the whole period of treatment. No significant trends indicating neither increase nor decrease in the values of estimated parameters were observed.

REFERENCES

1. Gralnic HR. Cancer cell procoagulant activity. In:Donati MB. Malignancy and the haemostatic system. New York:Raven Press;1981.p.57-61
2. Bratt G, Blombäck M, Paul C, Schulman S, Thornebohm E, Lockner D. Factors and inhibitors of blood coagulation and fibrinolysis in acute nonlymphoblastic leukemia. Scand J Haematol 1985;4:332-339
3. Renard N, Nooijen P, Schalkwijk L, DeWaal R, Eggermont A, Lienard D. VWF release and platelet aggregation in human after perfusion with TNF alpha. J Pathol 1995;176:279-287
4. Gran-Bassas ER, Kociba GJ, Couto CG. Vincristine impairs platelet aggregation in dogs with lymphoma. J Vet Intern Med 2000;1-2:81-85
5. Karolak L. High-dose chemotherapy induced platelet defect:inhibition of platelet signal transduction pathways. Am Molecul Pharm 1992;43:37-44
6. Bryan L, Mazey I. Corneal endothelial toxic effect secondary to fluorouracil needle bleeb revision. Arch Ophtal 1994;112:1411
7. Carey RV, Harris N. Thrombotic microangiopathy in three patients with cured lymphoma. Cancer 1989;7:1393-1397
8. Okazaki M, Znang H, Tsuji M, Morio Y, Oguchi K. Blood coagulability and fibrinolysis in streptozocin-induced diabetic rats. J Athero Thromb 1997;4:27-33
9. Addo-Boadu K, Wojta J, Christ G, Hufnagl P. Azelaic acid decreases the fibrinolytic potential of cultured human melanoma cell in vitro. Cancer Lett 1996;5: 125-129
10. Olman MA, Mackman N, Gladson CL Moser KM, Loskutoff DJ. Changes in procoagulant and fibrinolytic gene expresion during bleomycin-induced lung injury in the mouse. J Clin Invest 1995;9:1621-1630
11. Shan L, Kato Y, Kawana A, Jimbo A. Effect of phorbol ester on tissue-type plasminogen activator /tPA/ secretion in endometrial carcinoma cell line in vitro. Nippon Sanka Fujinka Gukkai Zasshi 1994;2:122-128
12. Marcum J, McGill M, Bastida E, Ordinas A, Jamieson GA. The interaction of platelets, tumour cells and vascular subendothelium. J Lab Clin Med 1980;6:1046-1053
13. Okrucká A. Zmeny hemostázy pri malígnych ochoreniach. Folia Fac Med Univ Comenianae Bratisl 1991;29:9-92
14. Lane DA, Ireland H, Wolff S, Ranasinghe E. Detection of enhanced in vivo platelet alpha-granuled release in different patients groups - comparison of beta-thromboglobulin,platelet factor 4 and thrombospondin assays. Thromb Haemost 1984;52:183-187
15. Rickles FR, Falanga A. Molecular basis for the relationship between thrombosis and cancer. Thromb Res 2001; 102:6:215-224
16. Kubisz P. Poruchy hemostázy pri nádorových ochoreniach. Lek Listy 2002;29:1-3
17. Galajda P. Vyšetrovanie porúch hemostázy u chorých s diabetes mellitus a inzulínovou rezistenciou. Lek Listy 1998;8:4
18. Filippi JF, Arnoux D, Tubiana N, Boutiere B, LeCaer F, Sampol J. Plasminogen activator activity of normal and malignant mononuclear human cells. Thromb Haemost 1987;1:105
19. Plowl EF, Plescia J. Neutrophil secretion during blood coagulation-evidence form precallicrein independent pathway. Thromb Haemost 1988:3:360-363.

Received: October, 22, 2002
Accepted: December, 6, 2002

ACUTE INFLUENCE OF THE ELECTROMAGNETIC FIELD ON THE HEART RATE VARIABILITY

Oto Osina[1], Jana Buchancová[2]

[1] Central Military Hospital, Department of Occupational Medicine and Toxicology, Ružomberok, Slovak Republic
[2] Department of Occupational Medicine and Toxicology, Comenius University, Jessenius Faculty of Medicine, Martin, Slovak Republic

Abstract

The aim of the study was to study an influence of the electromagnetic fields (EMF) on the autonomic nervous system (ANS) functions – regulation of the heart rate. Acute effects of the EMF (frequency 430 MHz) on the heart rate variability (HRV) were examined by spectral analysis in 30 healthy subjects. The input power of the EMF was 1 W and power density was 9.27 $\mu W.cm^{-2}$. The examination was performed under standard conditions. The HRV was recorded during 5 phases of examination given by a position of a proband (T1 – lying, T2 standing, T3 – lying, T4 lying + EMF, T5 lying). The duration of each phase was 5 minutes.

The statistical comparison of the values was performed between the values in the phases T3 and T4.

Total Power, Power VLF, Power LF, Power HF, Relative Power LF, MSSD, CCV VLF, CCV LF, CCV HF, LF/HF ratio - parameters of spectral analysis of the HRV and R-R intervals duration were increased in the phase T4 compared to the values in the phase T3. The effect persisted up to the T5 phase.

Spectral analysis of the HRV appears to be a sensitive method to monitor effects of the EMF on the regulatory ANS functions.

Key words: electromagnetic fields, autonomic nervous system, HRV, spectral analysis

INTRODUCTION

The electrochemical processes inside the living systems are sensitive to the influence of the external environment. We consider it necessary to identify not only these processes but also the factors which influence them. The electromagnetic fields (EMF) are the only ones from many factors which may influence electrochemical processes. At present the thermal effects of the EMF are well known, the non-thermal effects of the EMF are still slightly explained. At present, when hand transmitters and mobile phones are more frequently used, we can expect some disorders of the CNS functions, including autonomic nervous functions (ANS). This negative effect is little known and hasn't been definitely explained yet because of various features of the EMF (frequency, power density, modulation, locality of action and others) and of the biological systems and their subsystems (immunological, cardiovascular, ANS a.o.)

In this research we studied the influence of the EMF (frequency of 430 MHz) on the ANS functions by the spectral analysis of heart rate variability (SA HRV). We have chosen this frequency because it is almost like the frequency of non-modulated telecommunication systems (NMT – 450 MHz) and high-frequency transmitters of the rescue and safety services, etc.

METHODS

The used source of the EMF was remote operated portable radio transmitter Motorola. The used frequency was 430 MHz, input power was 1W and mean power density was 9.27 $\mu W.cm^{-2}$. The source of the EMF was placed close to a bed so that the top of the antennae was 3-4 cm from the right temporal part of a subject's head and 3 cm above the auricle. The examination was performed between 9.30 – 11.30 a.m. in a silent room with constant electromagnetic background. The mean temperature in the room was 24.06 ° C and mean atmospheric pressure was 95.8 kPa.

Address for correspondence:
Oto Osina, M.D., Central Military Hospital, Department of Occupational Medicine and Toxicology, Ul. gen. M. Vesela 21, 034 26 Ružomberok, Slovak Republic
Phone: ++ 421 44 4382 348
Fax: ++ 421 44 4382 682
e-mail: osina@uvn.sk

The microcomputer system VariaPulse TF4 (Sima Media Olomouc Ltd., Czech Republic) was used for registration and telemetric transmission of the R-R intervals to PC and for evaluation of the HRV parameters. The parameters of the heart rate variability (HRV) were determined by the means of Fast Fourier Transformation (FFT).

The examination was made in 5 intervals in the following algorithm – lying (T1) – standing (T2) – lying (T3) – lying with the EMF (T4) – lying without the EMF (T5). The duration of each time interval (T1 – T5) was five minutes. Parameters of the HRV in the T3 and T4 phases were analysed statistically by Student t-test.

The study was performed on 30 healthy, right-handed men at the mean age of 29.1 ± 4.95 (21 – 40), BMI 25.6 ± 2.8 with physiological values parameters of the HRV (LF and HF) during the T2 and T3 phases. Subjects had no abnormal physical and/or psychical load a day before the examination. All subjects were asked to avoid drinking coffee and alcoholic beverages and they slept for 6 and more hours a night before. Thirteen smokers among them haven't smoked for a minimum of 4 hours before testing. The subjects were informed about the silent switch on of transmitter but they did not know whether the source emits the EMF.

RESULTS

The characteristics of the group, conditions of the examinations and results of correlation analysis for Total Power (TP) between the TP and individual characteristics in the T3 and T4 phases are in Table 1.

Parameters of the frequency domain analysis of R-R intervals were compared to the standards which were found in the same age group in the hospital (Table 2) and they were evaluated in three frequency bands: The very low frequency band (VLF - 0.01 – 0.05 Hz) is related to thermoregulatory processes, vasomotor activities determined by the activity of sympathetic and hormonal systems. Its physiological correlates are still unknown. The baroreceptor activity is

Table 1. Characteristic of a group, conditions of examinations and results of correlation analysis for Total Power (TP) between the individual characteristics and TP in the phases T3 and T4

Characteristics	Mean values	SD ±	Correlation coefficient for TP in phase T3 (Lying)	Correlation coefficient for TP in phase T4 (Lying + EMF)
Age (years)	29.1	4.95	-0.33	-0.39
BMI (kg.m^{-2})	25.6	2.83	0.02	0.17
Systolic pressure (mm Hg)	124.5	8.02	-0.38	-0.24
Diastolic pressure (mm Hg)	81.5	3.7	-0.15	-0.12
The length of sleeping before testing (hours)	6.61	0.82	-0.04	-0.02
Time since last meal (hours)	14.5	3.35	0.15	0.14
Temperature inside the testing room (°CC)	24.06	0.69	0.21	0.21
Barometric pressure (kPa)	95.8	0.59	-0.02	0.13

Table 2. Reference value of VLF, LF and HF calculated for the age of 21 – 39 years (VLF – own measurement, LF, HF – Lacko (1))

Parameters HRV	Frequency (Hz)	Normal value in standing	Normal value in lying
VLF	0.01 – 0.05	15 – 315	24 – 385
LF	0.05 – 0.15	709 – 2115	400 –1500
HF	0.15 – 0.40	210 – 809	500 – 1930

reflected in the low frequency band (LF - 0.05 – 0.15 Hz) and includes both sympathetic and vagal influences. High frequency band (HF - 0.15 – 0.5 Hz) depends mainly on vagal activities (1, 2, 3, 4). Measurements of spectral activities in the VLF, LF and HF bands are usually given in absolute values of power (ms^2), relative values (in %) to the total power, coefficients of components variance (CCV in %) and the ratio between components VLF/HF, LF/HF, VLF/LF. The ratio of LF/HF is taken as an indicator of the sympathetic – vagal balance. Increased LF/HF ratio has been observed e.g. during 90° passive tilting, standing, mental stress and moderate exercise in healthy subjects (3, 5, 6, 7).

Time domain analysis of the R-R intervals is represented mainly by the MSSD parameter.

Table 3. The HRV parameters in the phase T3 (lying) and T4 (lying + EMF).
($p < 0.05$ - * significant difference).

Parameters SA HRV	T3 (lying)	SD ±	T4 (lying+EMF)	SD ±	Correlation coefficient between T3 and T4
Total Power (ms^2)	1344.9	784.9	**1745.6***	1069.9	0.71
Power VLF	221.3	175.8	299.4	276.9	0.54
Power LF	444.1	343.1	**662.2***	527.2	0.57
Power HF	679.6	452.3	815.9	537.6	0.61
Relat. Power VLF (%)	17.4	12.01	16.3	8.1	0.35
Relat. Power LF (%)	31.2	12.4	**36.9***	15.4	0.59
Relat. Power HF (%)	51.4	17.3	46.7	16.02	0.54
MSSD (ms^2)	1959.8	1515.5	2266.8	1678.7	0.86
CCV VLF	1.4	0.5	1.6	0.6	0.59
CCV LF	2.01	0.9	**2.42***	1.07	0.71
CCV HF	2.5	0.9	2.6	0.7	0.78
VLF/HF	0.49	0.5	0.41	0.2	0.54
LF/HF	0.8	0.7	**1.05***	0.9	0.84
VLF/LF	0.67	0.5	0.6	0.5	0.39
R-R interval (s)	0.98	0.1	**0.99***	0.1	0.96

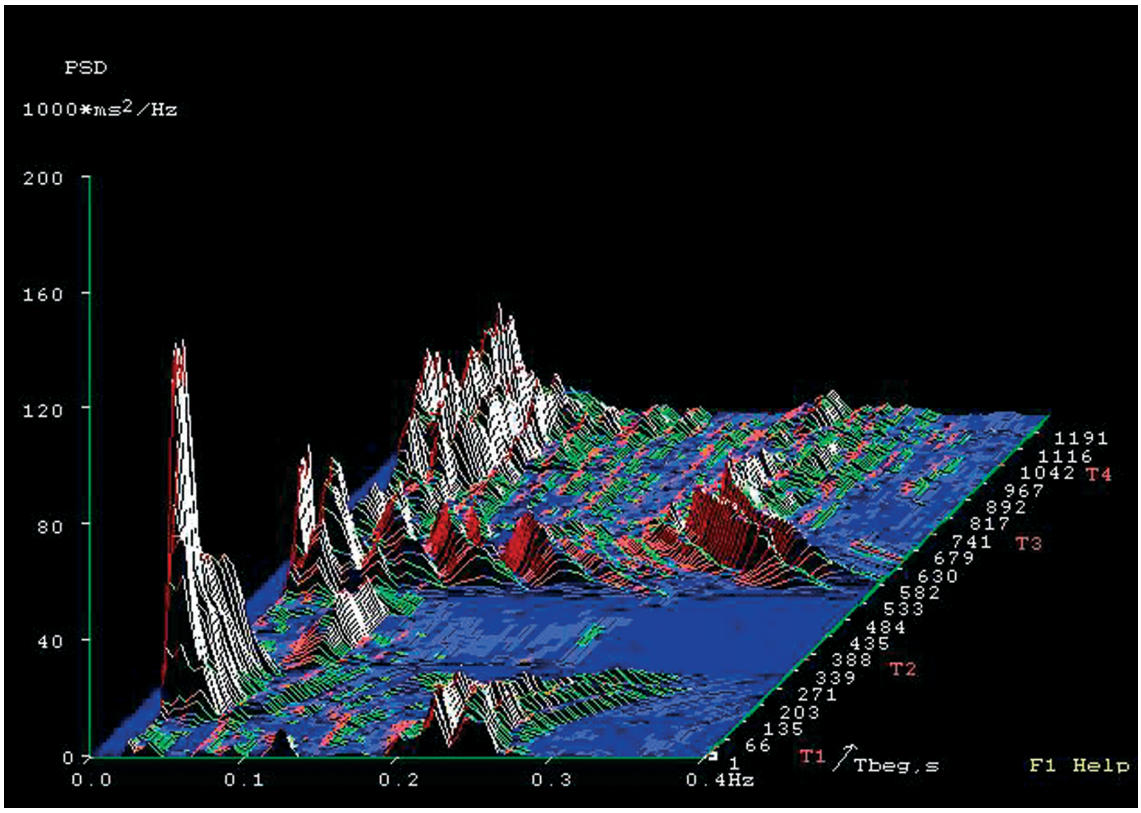

Fig. 1. Example of the SA HRV. On the axis **x** is frequency in Hz – (VLF: 0.01 – 0.05, LF: 0.05 – 0.15, HF: 0.15 –0.40), on the axis **y** power spectral density and on the axis **z** time – phases T1 – T4.

Figure 1 shows a typical finding of the LF activity increase and a concomittant decrease in the HF band during the T2 phase (standing) and the decrease in LF and a rise of the HF components in the phase T3. These reactions indicate the right function of ANS in heart rate regulation. In the phase T4 (lying + EMF) increase of LF and a decrease of HF components is evident. Table 3 shows mean values of evaluated parameters of the HRV. Starlets (*) indicate significant ($p < 0.05$) differences between values in T3 and T4. Graphic presentations of the results are in Fig. 2 and 3.

DISCUSSION

The electromagnetic field (EMF) from the receivers or mobile phones is absorbed mainly by anatomic structures of the head (skin, cranium). Only mild local increase of temperature was found in these parts of the head. The part of EMF depending on the frequency and power density, penetrates inside into the cranium and may influence the central nervous system including ANS through thermal effects. Additional adverse effects of the EMF can be developed by a thermal irritation of the superficial sensitive parts of n. facialis and n. vagus. Hypothalamic reactions can be responsible for another autonomic reactions consequently.

Spectral analysis of the HRV is an appropriate non-invasive test of heart regulation which identifies still early and light disorders of the regulation. Heart rate variability depends on several factors for example on breathing (8, 9, 10), blood pressure oscillations, thermoregulation, activity of the higher parts of CNS, etc. The HRV is a result of the sophisticated regulation through both parts of the ANS – sympathetics and parasympathetics. Both systems can be acti-

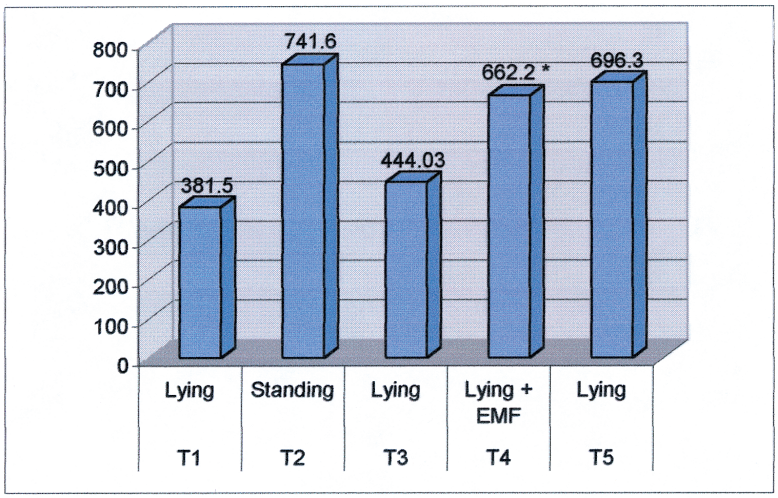

Fig. 2. Power LF values in the phases T1 – T5.

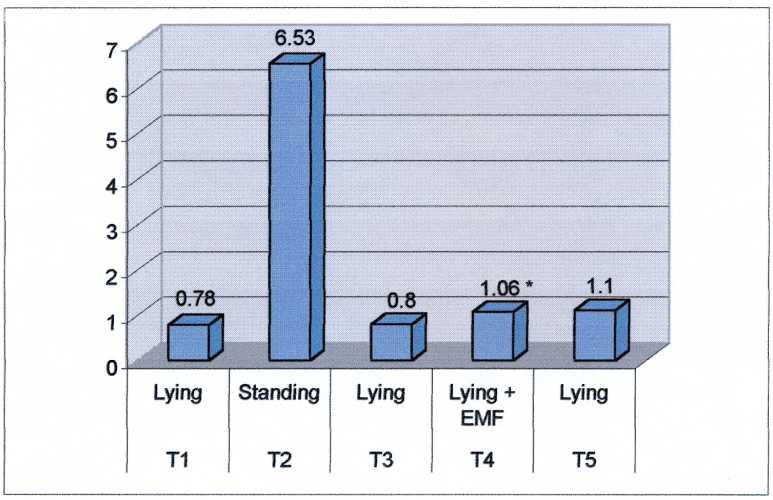

Fig. 3. The ratio LF/HF in the phases T1 – T5.

vated or inhibited separately or, more frequently, together in the dynamic balance way (3). HRV can also be influenced by environmental factors e.g. by a temperature (11, 12), atmospheric pressure, UV radiation or EMF.

The spectral analysis of the HRV is used to diagnose the ANS disorders in neurology, diabetology, cardiology and for evaluation of a prognosis after myocardial infarction (13, 14), etc. The HRV analysis was only rarely used for a study of the influence of risk factors in workplaces and for preventive early detection of the latent damages of the ANS. We suppose that the reasons are in the high sensitivity of the HRV on many factors e.g. age, BMI, sex, exhaustion, stress, actual health condition, meal, caffeine intake, smoking, exercise etc. (6, 7). From this point of view, we performed the examination at standard conditions with maximal elimination of disturbing factors. We calculated relationships between some factors and Total Power by means of the correlation analysis in the phases T3, T4. The results (Table 1) indicate there was not any important adverse influence of the factors on the parameters.

During the year 2002, we performed 93 examinations of the HRV in the subjects. Previously accepted criteria (mainly the right function of ANS – reactions in the phases T2 and T3) selected 30 of them. Statistical analysis of the heart rate parameters in the phase T3 – lying without influ-

ence of the EMF and in the following phase T4 – lying with application of the EMF was used for their comparison.

The results showed that in the phase T4 during the application of the EMF, the evaluated parameters of the HRV: Total Power, Power VLF, Power LF, Power HF, relative Power LF, MSSD, CCV VLF, CCV LF, CCV HF, LF/HF and R-R interval were increased. The changes were statistically significant mainly with the biggest difference in the LF band reflecting common sympathetic and vagal activities. The enhancement of LF/HF ratio indicates participation of a sympathetic reaction on the external stimulus – EMF. This enhancement and increase in LF parameters persisted also in the T5 phase. This increase could be explained by means of central heating effects of the EMF prolonged up to the 5th phase. It is well-known that normalization of the central temperature is a relatively slow process and the effect of the EMF can continue in this form also latter - in the following phase.

Our results support a hypothesis about the EMF influence on the CNS including ANS. The generalization of the results cannot be done because of the specific characteristics of the applied EMF. The verification of the results by using the frequencies close to 900 and 1800 MHz of mobile telecommunication systems could explain the different symptoms attributed to the EMF effects of mobiles phones.

CONCLUSION

Spectral analysis of the heart rate variability is applicable for detection of the ANS reactions on the internal and external factors including electromagnetic field. Application of the EMF increased spectral analysis parameters of the heart rate variability indicating a direct effect of the EMF on regulation of the heart rate by autonomic nervous system.

The study was a part of the Grant N.FVU 09/2001 realized between the years of 2001 – 2003.

REFERENCES

1. Lacko A. Bestvina D. Neinvazívna diagnostika kardiovaskulárnych ochorení. Vojenská akadémia v Liptovskom Mikuláši, 2001, 211pp.
2. Javorka K. Buchanec J. Javorková J. Buchancová J. Heart rate variability and physical fitness in children and adolescent with diabetes mellitus type 1. Int J Adolesc Med Health 2001; 13 (4): 297 – 309.
3. Javorka K. Metódy a prínosy vyšetrenia regulácie frekvencie srdca u detí. Čs Pediat 1996; 651 (8) : 462-468.
4. Kaliská D. Kmeč P. Autonomous nervous system testing in stratification of patients endangered by sudden heart death. Bratisl Lek Listy 1996;(97): 473- 478.
5. Javorka M. Žila I. Balhárek T. Javorka K. Heart rate recovery after exercise: relations to heart rate variability and complexity. Braz J Med Biol Res 2002; 35 (8): 991-1000.
6. Malik M. Bigger T. J. Camm A. J. Kleiger R. E. Malliani A. Moss A. J. Schwartz P. J. Heart rate variability, Standards of measurement. physiological interpretation, and clinical use. Europ Heart J 1996; 17: 354 – 381.
7. Tonhajzerová I. Javorka K. Javorka M. Petrášková M. Cardiovascular autonomic nervous system tests: Reference values in young people (15 – 19 years) and influence of age and gender. Clin Physiol Funct Imaging 2003 (in press)
8. Javorka M. Žila I. Javorka K. Čalkovská A. „Respiratory„ oscillations of cardiovascular parameters during voluntary apnea. Resp Physiol 2001; 126: 251-254.
9. Javorka M. Žila I. Javorka K. Čalkovská A. Do the oscillations of cardiovascular parameters persist during voluntary apnea in humans? Physiol Res 2002; 51: 227-238.
10. Javorka M. Approximate entropy – parameter kvantifikujúci komplexitu regulácie. Čsl Fyziol 2002;51 (1): 21-27.
11. Brozmanová A. Javorka K. Javorka M. Čalkovská A. Ševecová D. Petrášková M. Contribution of the parasympathetic system to respiratory and cardiovascular changes induced by both – experimental hyperthermia and its reversal. Acta Med Martiniana 2002; 2 (1) : 7-14.
12. Žila I. Brozmanová A. Javorka M. Čalkovská A. Javorka K. Chemical control of breathing in rabbits during hyperthermia. Abstracts of the 78th Physiol Days, SAV, Bratislava, 2002; p.81.
13. Opavský J. Salinger J. Vyšetřovací metódy funkcií autonomní nervové soustavy – přehled pro potřeby klinické praxe. Noninvas Cardiol 1995; (3): 139 – 153.
14. Krahulec B. Možnosti využitia kardiovaskulárnych reflexov v diagnostike porúch autonómneho nervového systému u nediabetikov. Nonivas Cardiol 1995; (3): 165 – 173.

Received: November,20, 2002
Accepted: January, 7, 2003

Instructions to authors for manuscripts submitted to ACTA MEDICA MARTINIANA

Journal Acta Medica Martiniana (AMM) publishes original papers of high quality from medical and biomedical sciences and from nursery, which have not been published yet, and will not be submitted for publication elsewhere. The papers are published in English, non-native English authors are responsible for the translation. The AMM is open access journal in print and online versions (http://www.jfmed.uniba.sk).

The Editorial Board of AMM requires the treatments of manuscripts in accordance with uniform requirements of biomedical journal editors (Vancouver, 1978 with the revisions in 1997 and 2000): Uniform Requirements for Manuscripts Submitted to Biomedical Journals:
http://www.icmje.org./index.html

Original papers in extenso should not exceed 15 pages (including references) and 5 figures or tables or their combination. The manuscript has to be written double-spaced (30 lines and maximum 60 keystrokes in a line per page) in the standard structure:

1. *The title page* (separately) should have the title of the article, full names of the authors, the name of department(s) or institution(s), full address of the corresponding author (including the phone, fax number and e-mail, if applicable).

2. Abstract (separately) in the extent of 1 standard page. Three to five key words are appended at the end of the abstract page.

3. *Introduction* should introduce into the problem and state the purpose of the article.

4. *Methods* should be complete to allow other workers to reproduce the results. Describe statistical methods. Indicate whether the procedure followed was in accordance with the ethical standards and with the Helsinki Declaration from 1975 as revised on 1983.

5. *Results:* Present your results in logical sequence in the text, tables and illustrations.

6. Discussion: Emphasize the new and important aspects of the study, link the conclusions with the presented goals of the study, relate the results to other relevant studies with a short summary of results at the end.

7. *References:* All publication cited in the text should be presented in references. References have to be numbered consecutively in the order in which they are first mentioned within the text. Identify references in the text by Arabic numerals in parantheses. Use abbreviations of the journals according to Index Medicus (List of Journal Indexed in Index Medicus, http://www.nlm.nih.gov).

Examples as follow (other examples are included on the web page being mentioned):

Article in Journal: Vega KJ, Puna I, Krevsky B. Heart transplantation is associated with risk for pancreatobiliary disease. Ann Intern Med 1996; 124 (11): 980-3.

Books and other Monographs: Bond J. Ageing of a spy. New York: Churchill Livingstone; 1999.

Chapter in a book: Phillips SJ, Whisnant JP. Hypertension and stroke. In: Laragh JH, Brenner BM, editors. Hypertension: pathophysiology, diagnosis, and management. 2nd ed. New York: Raven Press; 2001. p. 465-78.

Illustrations and tables: Letters, numbers and symbols should be sufficient size that when reduced for publication each item will still be legible. Type legends for illustrations on a separate page. Each table has to be on a separate page too. Place explanatory matter in footnotes. Vertical rules should be omitted. Figures and tables should be numbered consecutively according to the order in which they have been first cited in text.

Units of Measurement and Symbols: Measurements of length, height, weight, and volume should be reported in metric units. Temperatures should be given in degrees Celsius, blood pressure in millimeters of mercury. All other measurements should be reported in the terms of the International System of Units (SI).

One complete original manuscript with one set of high-quality prints of the figures and two complete copies, each containing tables and copies of the figures, must be submitted to the address of the Editorial Board Office.

All manuscripts will be peer-reviewed anonymously by external experts pursuant to the standard evaluation criteria. Based on the review opinions, the Editorial Board will decide, whether the paper is to be included in the journal.

After a manuscript is accepted for publication, one hardcopy of the final revised, accepted version of the paper must be submitted along with the same version on a 3.5-in. diskette. Text files should be saved as word processing document using Microsoft Word. The manuscipt has to include an attachment as follows: *The work is an original, which has not been published in its full extent yet and will not be submitted elsewhere before a decision has been taken as to its acceptability by Acta Medica Martiniana. In consideration of the acceptance of the above work for publication, I do hereby assign and transfer to the publisher the copyright including display of the article in electronic form on web (open access).*

Publication of articles is free of charge.

AMM Editorial Board
Dept. of Physiology Jessenius Medical Faculty
Comenius University
Mala Hora Str. N. 4
037 54 MARTIN
SLOVAKIA